AFAMRL-TR-80-27

INVESTIGATION OF PHOTOGRAPHIC IMAGE QUALITY ESTIMATORS

GILBERT G. KUPERMAN

APRIL 198

Approved for public release; distribution unlimited.

AIR FORCE AEROSPACE MEDICAL RESEARCH LABORATORY
AEROSPACE MEDICAL DIVISION
AIR FORCE SYSTEMS COMMAND
WRIGHT-PATTERSON AIR FORCE BASE, OHIO 45433

NOTICES

When US Government drawings, specifications, or other data are used for any purpose other than a definitely related Government procurement operation, the Government thereby incurs no responsibility nor any obligation whatsoever, and the fact that the Government may have formulated, furnished, or in any way supplied the said drawings, specifications, or other data, is not to be regarded by implication or otherwise, as in any manner licensing the holder or any other person or corporation, or conveying any rights or permission to manufacture, use, or sell any patented invention that may in any way be related thereto.

Please do not request copies of this report from Air Force Aerospace Medical Research Laboratory. Additional copies may be purchased from:

National Technical Information Service
5285 Port Royal Road
Springfield, Virginia 22161

Federal Government agencies and their contractors registered with Defense Documentation Center should direct requests for copies of this report to:

Defense Documentation Center
Cameron Station
Alexandria, Virginia 22314

TECHNICAL REVIEW AND APPROVAL

AFAMRL-TR-80-27

This report has been reviewed by the Office of Public Affairs (PA) and is releasable to the National Technical Information Service (NTIS). At NTIS, it will be available to the general public, including foreign nations.

This technical report has been reviewed and is approved for publication.

FOR THE COMMANDER

CHARLES BATES, JR.
Chief
Human Engineering Division
Air Force Aerospace Medical Research Laboratory

AIR FORCE/56780/15 July 1980 — 150

SECURITY CLASSIFICATION OF THIS PAGE (When Data Entered)

REPORT DOCUMENTATION PAGE

READ INSTRUCTIONS BEFORE COMPLETING FORM

1. REPORT NUMBER: AFAMRL-TR-80-27	2. GOVT ACCESSION NO.: AD-A087 805
3. RECIPIENT'S CATALOG NUMBER:	
4. TITLE (and Subtitle): INVESTIGATION OF PHOTOGRAPHIC IMAGE QUALITY ESTIMATORS	5. TYPE OF REPORT & PERIOD COVERED: Technical Report
6. PERFORMING ORG. REPORT NUMBER:	
7. AUTHOR(s): Gilbert G. Kuperman	8. CONTRACT OR GRANT NUMBER(s):
9. PERFORMING ORGANIZATION NAME AND ADDRESS: Visual Display Systems Branch, Human Engineering Division, Air Force Aerospace Medical Research Laboratory	10. PROGRAM ELEMENT, PROJECT, TASK AREA & WORK UNIT NUMBERS: 62202F, 7184-11-32
11. CONTROLLING OFFICE NAME AND ADDRESS: Air Force Aerospace Medical Research Laboratory, Aerospace Medical Division, AFSC, Wright-Patterson Air Force Base, Ohio 45433	12. REPORT DATE: April 1980
	13. NUMBER OF PAGES: 112
14. MONITORING AGENCY NAME & ADDRESS (if different from Controlling Office)	15. SECURITY CLASS. (of this report): Unclassified
	15a. DECLASSIFICATION/DOWNGRADING SCHEDULE

16. DISTRIBUTION STATEMENT (of this Report)

Approved for public release; distribution unlimited.

17. DISTRIBUTION STATEMENT (of the abstract entered in Block 20, if different from Report)

18. SUPPLEMENTARY NOTES

Funding for this study was provided by the AFAMRL Laboratory Director's Fund as LDF 79-4.

19. KEY WORDS (Continue on reverse side if necessary and identify by block number)

Resolving Power
SENTINEL SIGMA
Modulation Transfer Function
Quality Assurance
Acutance
Math Model
Film Threshold

20. ABSTRACT (Continue on reverse side if necessary and identify by block number)

Three predictors of photographic image quality, Inverse Square Law (ISL), Modulation Transfer Function (MTF), and Sun's Equation, were compared against two subjective techniques: Resolving Power (RP) and Visual Image Evaluation (VIE), and five objective techniques: Acutance, Edge Width, Reciprocal Edge Spread (RES), and two MTF/Aerial Image Modulations (MTF/AIM). Tribar targets at four nominal contrast levels were photographed while the film plane was driven through 7 1/2 cycles of sinusoidal image motion at seven peak-to-peak

DD FORM 1 JAN 73 1473 EDITION OF 1 NOV 65 IS OBSOLETE

SECURITY CLASSIFICATION OF THIS PAGE (When Data Entered)

(20 continued)

displacement amplitudes, 0.00000 (i.e., static), 0.00025, 0.00050, 0.00075, 0.00100, 0.00125, and 0.00150 inches. An analysis of variance (ANOVA) was performed for the RP data. Targets, Amplitudes, and their interaction were found to be highly significant ($p < 0.01$). The independent variables and their interactions accounted for over 96 percent of the total experimental variance. The three predictive models (ISL, MTF, and Sun's Equation) all were highly correlated ($r > 0.96$) linear functions of RP. The VIE technique also proved to be a highly linear correlate of RP ($r = 0.95915$). The ANOVA for VIE yielded highly significant ($p < 0.01$) results for Subjects, Targets, Amplitudes, the Subjects × Targets, and the Subjects × Amplitudes interactions, and significant ($p < 0.05$) differences for the Targets × Amplitudes interaction. The independent variables and their interactions in the VIE ANOVA accounted for over 87 percent of the total experimental variance. The objective techniques yielded results which were not significantly different from each other but were poor correlates (r between 0.45 and 0.65) of RP.

SUMMARY

The United States Department of Defense relies on aerial photography as a major resource in satisfying intelligence and mapping requirements. The Air Force has instituted a quality assurance program for photographic collection systems and established requirements for developing nominal performance standards for each such system. This report documents a series of studies in which predictive models and objective and subjective image quality assessment methods were compared against each other using photography that had been subjected to multiple cycles of sinusoidal image motion.

PREFACE

The research described in this report was conducted by the Visual Display Systems Branch, Human Engineering Division, Air Force Aerospace Medical Research Laboratory. The research was performed under Project 7184, "Man-Machine Integration Technology"; Task 7184 11, "Design Parameters for Visual Display Systems"; Work Unit 7184 11 32, "Investigation of Photographic Image Quality Estimators." Funding for this study was provided by the AFAMRL Laboratory Director's Fund as LDF 79-4.

The author wishes to thank the following individuals for their support of and contributions to the accomplishment of this research: Mr. James C. Haley, Chief, Dynamics and Environmental Evaluation Branch, Reconnaissance and Weapon Delivery Division, Air Force Avionics Laboratory, who provided encouragement for the initiation of this effort and who, together with Mr. Edward Gliatti and Mr. Thomas Stanzione of his branch, strongly contributed to this research by providing stimulus materials, making trained subjects available, and performing microdensitometry and image quality analyses during the data collection phase; Mr. John Ream, Mead Technology Laboratories, Dayton, Ohio, who directed a portion of the modulation transfer function analysis; Mr. Joseph Fragiotti of Systems Research Laboratories, Inc., Dayton, Ohio, who assisted in performing the predictive analysis; and Mr. Anthony DeFrances and Mr. Kevin Holloran, Systems Research Laboratories, Inc., for assisting in the performance of the statistical analyses.

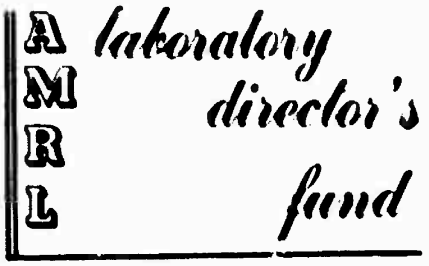

TABLE OF CONTENTS

TABLE OF CONTENTS (continued)

LIST OF ILLUSTRATIONS

LIST OF ILLUSTRATIONS (continued)

LIST OF ILLUSTRATIONS (continued)

LIST OF TABLES

Section 1
INTRODUCTION

QUALITY ASSURANCE PROGRAM

Air Force Regulation 96-1, "Quality Control Requirement for Continuous Photographic Processing Laboratories," stresses that "imagery-recording systems continue to provide one of the major sources of information to satisfy intelligence and mapping requirements." It further states that "the maximum information must be obtained from the acquired imagery," which "requires that each component of the reconnaissance or mapping cycle be considered in terms of its possible effect on the other aspects of the cycle" and that "controls must be established to minimize degrading effects." In discussing the interrelationship between acquisition system components, the Regulation points out that "one limiting factor in product quality is the performance capability of the sensor and vehicle system combination. Each sensor has a specific image capability. This capability reflects the operation of the system under ideal conditions. In practice, however, the performance of a sensor system is influenced by operator and maintenance variables, climatic conditions, vibration, sensor mount, and sensor windows. These factors can degrade the quality of the imagery." The Regulation provides criteria for categorizing Air Force laboratories, based on their capabilities to support different levels of mission requirements. Each of the three categories of photographic laboratories is charged with an image evaluation responsibility commensurate with its organic capabilities as follows:

a. Category "A" facilities:

(1) Perform imagery evaluations to determine if the acquisition system operated satisfactorily as compared to design specifications and identify possible limiting components.

(2) Utilize primarily objective analytical techniques requiring highly specialized equipment including mensuration devices, viewers, microdensitometers, and computers.

(3) Perform detailed analysis on at least five percent of the missions from each reconnaissance and mapping program within 3 months after receipt of the imagery.

b. Category "B" facilities:

(1) Perform imagery evaluations to determine that the nominal performance standards for each reconnaissance or mapping program are being obtained.

(2) Utilize analytical techniques requiring some specialized equipment, including sophisticated viewing equipment, some image mensuration devices, and minimum computational support (such as desk calculators).

c. Category "C" facilities:

(1) Perform imagery evaluations to determine the causes of degradations in image quality so that corrective action can be taken.

(2) Utilize subjective analytical techniques requiring little specialized equipment.

(3) Perform imagery evaluation on all missions from each reconnaissance and mapping program within 20 hours after receipt of the film.

The three categories of laboratory facilities are directly comparable with the three levels of exploitation called out in the Defense Intelligence Manual (DIAM 57-5) DoD Exploitation of Multi-Sensor Imagery. Thus, a Category "A" facility would provide third phase interpretation for direct support requirements, a Category "B" facility would support collection system imagery intended for detailed evaluations such as Supplemental Photographic Interpretation Reports (SUPIR), while a Category "C" facility would perform quality controlled processing and duplication of reconnaissance imagery intended for Immediate Photographic Interpretation Reports (IPIR). (Additional information on imagery interpretation reporting requirements can be found in AFM 200-50, Image Interpretation Handbook.)

NOMINAL PERFORMANCE STANDARDS

AFR 96-1 serves to establish the minimum requirements of a United States Air Force Imagery Evaluation Program. Each major command which supports reconnaissance or mapping imagery acquisition is tasked with implementing this program. Further, responsibility is assigned "to accomplish evaluations related to system performance in support of all reconnaissance and mapping programs for which the U.S. Air Force has system development responsibility" and "for developing nominal performance standards for each USAF reconnaissance or mapping program." Crane (1975 and 1976) emphasized that "a key element of the USAF Imagery Evaluation Program is the formulation of a Nominal Performance Standard (NPS) for each USAF Reconnaissance/Mapping System." The NPS was seen to be a "key objective" of the Air Staff-initiated Project Sentinel Sigma. Crane voiced the expectations of the Assistant Chief of Staff for Intelligence, Headquarters USAF, that "the NPS will specify, in terms of image quality, the operational performance of any given sensor/film/aircraft combination," that "it will directly relate to the quality of the imagery the analyst/interpreter requires from operational missions," and "that the NPS can provide a common term of reference among USAF systems development, logistics and operational personnel, as well as a common technical baseline among the USAF, other DoD military departments and agencies, and industry."

The development of NPS-type figures of merit is a critical and nontrivial undertaking. As has been noted, the inherent image quality of photographic acquisition systems can be degraded by a number of external influences. The measurement techniques available at each operational level cannot be assumed on an a priori basis to provide equivalent validity or robustness in the face of such perturbations. (The purpose of this investigation is to achieve a better understanding of the comparative capabilities of objective [machine-oriented] and subjective [man-centered] image quality assessment techniques in application to high resolution photographic systems that have been degraded by well-controlled sinusoidal motions.)

STANDARDS FOR IMAGE QUALITY EVALUATION

The Defense Intelligence Agency is attempting to satisfy the need for image assessment procedures through the preparation and publication of standard procedures. The first of these, titled "Standardized Assessment and Expression of Tribar Resolution," discusses the need for such systems analysis in some detail:

> Imaging systems continue to provide one of the primary sources of information used to satisfy U.S. intelligence requirements. However, the cost and complexity of developing and utilizing these systems have increased enormously in recent years. Consequently, it is imperative that the development, operation, processing, handling, and exploitation of each imagery system be accomplished in a manner that allows the maximum information potential derivable from the system to be realized. One of the primary means for achieving this goal is through the systematic analysis of the actual imagery acquired by each reconnaissance mission to determine whether or not the quality of the imagery is considered to approach the level expected, with due regard to all of the factors which can influence image quality. If the quality is not as good as expected, then steps must be taken to determine the nature and cause of the degradation so that appropriate corrective action can be taken. In addition to evaluating "operational" imagery, as a means of monitoring the performance of the imaging system, the film processing, and related activities, the periodic analysis of "test" imagery also can provide the basis for calibrating certain system components, film processors and printers, film handling techniques, and numerous other aspects of the imagery collection/processing/exploitation cycle.

The variety of systems parameters is also discussed, and the reasons for initiating the series of Image Quality Assessment Standards, with one treating tribar resolution, are presented as follows:

> The analysis of image quality involves the assessment of various parameters, including density, contrast, "edge" sharpness, granularity, and resolution. To insure the data derived from this analytical process are valid and useful, standardized techniques and procedures should be used. This has not been the case historically, resulting in a profusion of data that is often of little value or even misleading. As a result of this situation, an effort is being made within the U.S. intelligence community to standardize some of

the more commonly used imagery evaluation techniques. "Photographic resolution" is probably the most commonly used method of quoting system performance. In fact, it is utilized in a variety of ways, including the development and calibration of optical components within the sensor system and the calibration of processing/printing equipment in the photographic laboratory, as well as for measuring the quality of the actual imagery products derived from operational reconnaissance missions. It is for this reason that "resolution" has been addressed initially in the current effort to standardize imagery evaluation techniques.

This document [the tribar standard] was thus conceived and designed to standardize procedures used by U.S. intelligence activities in the assessment and expression of photographic resolution. The initial problem was to decide which of the several methods currently used to determine resolution should be first standardized. "Tribar" resolution was selected because it is the most commonly used and misused.

Other resolution measuring techniques, some of which are still in the research and development stage, are under consideration and may be addressed at a future time.

Thousands of tribar resolution target readings are often necessary for the test and qualification of a new camera system. While the number of readings may be reduced as new resolution determination procedures are developed, the current level of dependence on tribar resolution data will continue for the foreseeable future. Among their many applications, tribar resolution data influence system acceptance, estimates of system performance, and statements of image quality. Thus, the data are important to the imagery acquisition and imagery exploitation communities alike. It is therefore imperative that the reported values be accurate, precise, and independent of reader, equipment, and organizational bias. It is not too strong a statement to say that these conditions have not always been met; this standard is intended to overcome this situation.

PURPOSE OF PRESENT RESEARCH

The intent of the investigations reported herein was twofold. First, it was hoped that a better understanding of the effects of sinusoidal vibration on photographic image quality could be achieved. Second, it was hoped that a comparison of the image quality estimators themselves would prove useful to the Air Force in identifying specific techniques for each of the three

categories of laboratory facilities and that the results produced by the several methods would prove mutually relatable.

The report has been prepared from the standpoint of a research psychologist and is not intended to be an exhaustive review of image quality assessment research. Where appropriate, previous research is specifically cited in the descriptions of the techniques and procedures, and more general or detailed references are also identified.

Section 2
IMAGE QUALITY ESTIMATORS (SUBJECTIVE)

This section presents and discusses the two subjective methods of image quality assessment applied in this research, Resolving Power and Visual Image Evaluation. By subjective, the author means that the image is sampled by the human perceptual system (rather than by a microdensitometer) and that the judgment reported as the response parameter is arrived at cognitively (rather than computationally).

A variety of tribar target designs and applications is presented, and resolving power, the associated dependent measure, is defined. Some of the strengths and weaknesses of this image quality estimator are identified in the context of the research literature. A similar development is presented for the Visual Image Evaluation technique.

TRIBAR TARGETS

Military Standard

Military Standard 150A (1959) defines the tribar target by the following geometric specifications:

1. "The target shall consist of a series of patterns decreasing in size as the $\sqrt{2}$, $\sqrt[3]{2}$, $\sqrt[6]{2}$, with a range sufficient to cover the requirement of the lens-film combination under test.

2. "The standard target element shall consist of two patterns (two sets of lines) at right angles to each other.

3. "Each pattern shall consist of three lines separated by spaces of equal width.

4. "Each line shall be five times as long as it is wide." (See Figure 1.)

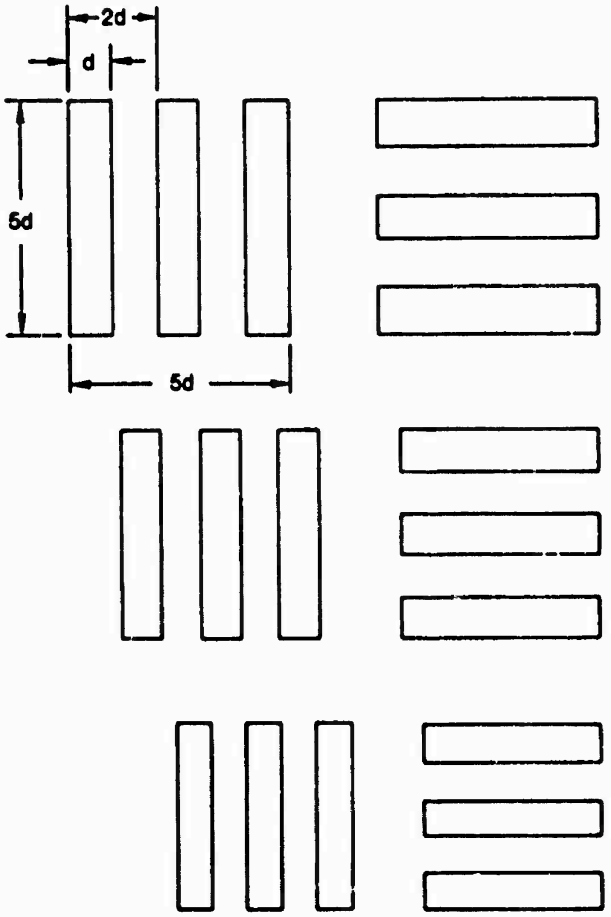

Figure 1. Sample Patterns from a Military Standard Tribar Target

The target contrast is defined in terms of the (photographic) density difference between the lines (bars) and spaces. A high contrast target is specified as providing a density difference greater than 2.00. A medium contrast target has a density difference of 0.80 ±0.05 and a low contrast target exhibits a density difference of 0.20 ±0.05.

USAF 1951

This target is a Military Standard configuration which follows a sixth-root-of-two progression. (This means that the line width doubles with each seventh pattern.) It is arranged in groups of six elements with a group number at the head of each group and an element number adjacent to each element within the group to facilitate reporting. A typical USAF 1951 target might exhibit elements from Group -2/Element 1 (0.25 cy/mm) through Group 7/Element 6 (228 cy/mm). (Other laboratory targets used for processing and duplication control are described in the DIA Manual.)

Fixed Tribar Targets

Tribar targets are used outside the laboratory to support flight test assessments of photographic acquisition system performance. Large, permanent targets have been constructed at several installations across the country including Wright-Patterson AFB and Edwards AFB. The Edwards AFB Low Range contains, for example, 14 tribar targets which are (nominally) identical in geometric design and contrast. These targets follow a sixth-root-of-two progression from a largest bar, whose width is 30.25 inches, to a smallest bar, whose width is 1.19 inch. The contrast of this type of target is specified as the ratio of the reflectance of the white bar to the dark background.

Mobile Tribar Targets

Military Standard 105A and nonstandard designs have been fabricated as portable targets. An example of a nonstandard design is the 51/51 Tribar Target. It exhibits a 5:1 aspect ratio (bar length to width) and a (nominal) 5:1 contrast (reflectance ratio). Instead of having the two orthogonal patterns of each element adjacent to each other, the target is physically divided into two "legs." Each leg contains patterns which progress by the sixth-root-of-two (with the exception of the two lowest patterns on each leg). All lines on the same leg are parallel to each other. The two legs are displayed perpendicular to each other in use. Each leg is 381 feet long. Bar widths range from 96 inches to 0.56 inch. (Descriptions of other

laboratory and field targets are provided in both the DIA and Controlled Range Network Manuals.)

RESOLVING POWER

The dependent measure estimated through the exploitation of tribar targets is termed resolving power (RP). With respect to the tribar target, Military Standard 150A (1959) defines RP as the "ability to image closely spaced objects so that they are recognizable as individual objects" and its measurement as the "reciprocal of the center-to-center distance of the lines that are just distinguishable in the recorded image." The unit used to express RP data is cycles per millimeter (cy/mm) where one cycle corresponds to twice the bar width.

Katz (1963) recalls that the introduction of tribar targets into camera testing in 1941 offered a quality control procedure that had "some relation to the picture-taking community out in the field--the aerial reconnaissance users." Brock et al. (1966) stressed that RP estimates have been made for many years and "have a commonly understood meaning throughout the photo-optical community," and Mayo (1968) noted that it is the "most commonly used criterion." In 1970, Brock pointed out the appropriateness of RP to estimate the capabilities of cameras used against the rather specific objectives of aerial reconnaissance. Higgins (1977) and others have noted that RP is not necessarily a good predicator of image quality and pointed out that "in some cases [it] may be misleading." Dainty and Shaw (1974) state that "it is clear that resolving power is not merely a measure of the ability of the photographic layer to record fine detail; rather, it is a measure of the complete lens/photographic/microscope/visual system, and the overall ability to detect special types of signal in image noise." (Other discussions of the advantages and disadvantages of RP measurements are found in Brock, et al., 1966; Noffsinger, 1970; and Attaya et al., 1966.)

REVIEW OF RP STUDIES

As has been noted, the application of RP measurement as an image quality assessment methodology has been pursued for at least 35 years. The findings

reported from other studies will serve as a background to the results of the present experiment.

Pittman (1965) performed an analysis on the RP evaluation of three aerial reconnaissance films. Tribar targets, at seven target contrasts, were imaged under highly controlled optical conditions. Three subjects (Ss) read the RP values. Pittman's conclusions are summarized:

1. The 99.7 percent confidence limits about the mean RP thresholds were from 2 to 6 percent of the means themselves.

2. Significant reader differences were demonstrated for both means and variability.

3. Significant reader-by-target contrast interactions were found.

4. Standard deviations for individual films were 7 to 11 percent for one type and 10 to 18 percent (of the mean) for the other two films.

In the Final Technical Report on the four-year program, which included Pittman's emulsion RP measurements, Attaya et al. (1966) strongly advocate the application of analysis of variance to the study of RP data. They close their discussion of this topic by stating that "in summary, it is hard to escape the conclusion that the most serious current problem in resolution practices is the serious general lack of recognition of the statistical nature of resolution."

Charman and Olin (1965) included the results of a study on RP as a function of lens field angle in their tutorial on image quality criteria. Using four Ss to determine RP at 10 format positions, they found differences between readers and between replicate readings by the same observer. They noted that the differences between individual readers of the same tribar image resulted in standard deviations equal to about 14 percent of the mean.

Mayo (1968) reported on two RP studies. In the first experiment, using three Ss, reader differences and reader-by-target contrast interactions were found. The second experiment used six Ss. Ss were found to group, based on RP readings, with about ± 12 percent difference in the means of two groups, but with each group being self-consistent to within about 6 percent of the mean. Overall, the standard deviation was found to be approximately 12 percent and Mayo concluded that "all factors considered, no resolving power determination should be assumed more reliable than ±10 percent of the measured value, based on reader differences alone."

VISUAL IMAGE EVALUATION

This method was apparently first proposed by Lt. Col. K. Saunders (then AF/XOOWAO) in about 1970. He summarized this concept as follows:

> The primary means . . . for evaluating photographic quality involves the use of resolution targets. Another system . . . is to determine the number of times the negative film can be enlarged and printed before the image begins to "break up." A possible solution . . . would be to determine the enlargement or magnification factor of the imagery . . . through the use of an adjustable, high powered microscope.

This technique, then, was intended to provide an alternative to RP estimates without requiring the presence of resolution targets. It was based on the observation that photographic grain (and other physical characteristics) place a limitation on the maximum usable magnification factor achievable in photographic enlargement and printing. In fact, the first name for his proposed technique was Maximum Magnification Factor (MMF), with the terminology Visual Image Evaluation (VIE) coming into usage only during the past 2 years. Gliatti (1978) provided a brief description of the method for obtaining MMF estimates:

> The procedure used is to view the imagery using a variable magnification zoom binocular microscope. The imagery is magnified to a point of empty magnification; i.e., where no additional information is obtained with increased magnification; in fact, information is lost due to grain, limited image resolution, motions during exposure, image contrast and/or

> other degrading factors. On a frame many MMF readings are made in an area and the average magnification recorded.

A very limited study of the utility and robustness of the VIE approach was performed by HRB-Singer, Inc., for the Rome Air Development Center in 1971. Only five frames of imagery were used. Photographic resolving power for the imagery used in the test was in the range 7.3 through 31.3 cy/mm. No significant correlation between VIE and RP was found. A second evaluation of the technique was performed at the Tactical Air Warfare Center (TAWC) under Project 1125 and reported in the 1972 Constant Quality final report. TAWC found that:

> No correlation between MMF and resolution could be established that would be useful to tactical image quality analysis. Individual differences compounded by contrast variance, scale variance, and target type are critical problems which could not be adequately defined or categorized using typical tactical imagery.

Despite the discouraging results of these early studies, attempts to apply the VIE technique continued. Several problem areas appeared to require solution. Readers, particularly tactical imagery interpreters, were not sufficiently experienced in performing RP readings required for VIE comparison or in exploiting optical magnifications greater than about 10 diameters. The third problem appeared to be that of individual differences, cited by the TAWC study. The DIA Standard for RP readings includes a training and certification procedure which supports the development of stable RP estimates and provides experience in using higher optical magnifications. The problem of individual differences has been addressed through the use of a multiplicative correction factor for each reader. The 1978 (draft) revision of the Image Quality section of T.O. 10-1-6-2 provides essentially the same procedure as was given by Gliatti (1978) and also describes a way to correct for individual differences and make the resulting reading correspond directl with RP values:

> For each reader, there is a different level at which "Empty Magnification" occurs. Thus a factor must be established for

each individual on each system. The majority of factors range from 1.8 to 2.3. Initially, a factor of 2 is used until the reader establishes his true factor.

Section 3
IMAGE QUALITY ESTIMATORS (OBJECTIVE)

Four basic machine-based estimators of image quality were employed in this research. They were acutance, edge width, reciprocal edge spread, and the modulation transfer function. Each is defined and described below.

ACUTANCE

Edges abound in both natural and cultural scenes. Mathematically, an edge (target) is a Heaviside Function, H(x), which is defined as:

$$H(x) = \begin{cases} 0, \text{ for } X \leq X_i \\ \\ 1, \text{ for } X > X_i \end{cases}$$

where H(x) is in reflectance. If a photographic system were perfect, then an edge target (reflectance) would be recorded as an edge target (density). In practice, such an input results in the creation of a recorded image in which the transition between density levels is not a perfect Heaviside function. If the edge exposure were perturbed (only) by linear motion, for example, the resulting distribution would be a "ramp," having constant, finite slope. Images created by these two systems (i.e., perfect and degraded by motion) would, presumably, be easily distinguishable by observers, with the motion-degraded photograph appearing to be "less sharp." In fact, such judgments, including ranking, have been made. Scott (1968) reported that "observers can just distinguish approximately 5 percent differences in the size of the spread functions of grainless photographs of identical scenes; for grainless photographs of different scenes, observers distinguished the spread function size with 10 percent sensitivity." Obviously, then, perceived sharpness is a dimension along which one can measure image quality. Acutance is an objective correlate to the subjectively judged sharpness parameter.

Biberman (1973) describes acutance as being "expressed in terms of the mean square of the gradient of . . . density (in a photographic image) with

distance from the edge." Both Biberman and Thomas (1973) provide the same formulae and procedure. The following procedure is extracted from Thomas:

1. Locate the endpoints (A and B) of the geometric edge.

2. Divide the distance between A and B into small, equal intervals, ΔX_i

3. Measure the density difference ΔD_i for each interval from the (smoothed) microdensitometer trace (calibrated in density units).

4. Compute the gradient $\frac{\Delta D}{\Delta X_i}$ and square it for each interval.

5. Compute the quantity $\left[G_x^2\right]_{av}$ where

$$\left[G_x^2\right] = \frac{\sum\left(\Delta D_i / \Delta X_i\right)^2}{n}$$

and n is the number of intervals.

6. Normalize against the density range DS corresponding to A and B and compute acutance:

$$\text{Acutance} = \frac{\left[G_x^2\right]}{DS}$$

Gliatti (1978) and Attaya and Yachik (1971) report on the application of acutance in the laboratory. Roetling, Trabka, and Kinzly (1968) relate it to the MTF-based equivalent passband. Kress and Gliatti (1977) describe the procedure used in support of the present research.

EDGE WIDTH/RECIPROCAL EDGE SPREAD

It is intuitively appealing to relate a directly observable feature of the microdensitometer scan (trace) across an edge to the image quality of the system. This has been adopted into practice through the use of two measures, the edge width and the reciprocal edge spread. The edge width is the

physical distance between the minimum and maximum density levels of the recorded edge and is expressed in microns.

Transfer function analysis relates image quality to interpreter performance. Roetling, Trabka, and Kinzly (1968), for example, noted that "the transfer function response at a spatial frequency corresponding to the reciprocal of an object size is often used to estimate the detectability of an object." A similar argument appears to underlie the derivation of the reciprocal edge spread (RES) as an image quality assessment. The edge width is inverted and multiplied by the constant 1000 (microns per millimeter) to obtain a value that is expressed in cycles per millimeter, i.e., directly comparable to RP. Kress and Gliatti (1977) show the use of both the edge width and the reciprocal edge spread.

MODULATION TRANSFER FUNCTION (MTF)

The analytic and practical application of linear systems theory has been well established for electrical communications systems. A natural extension occurred with the replacement of temporal frequency response (of use in electronic engineering) by the parameter of spatial frequency response, which is of significance to the photographic systems designer/evaluator. The advent of rapid computational methods, particularly the Cooley-Tukey algorithm, and their continued improvement (e.g., Gold and Rader, 1969) have supported their widespread application. Several sources provide excellent and rigorous mathematical developments for the MTF. (The author follows Dainty and Shaw, 1974, in making the following observations.)

The photographic system is assumed to be both linear and stationary. Linearity requires that if a complicated input (e.g., a target's exposure distribution) is decomposed into simple inputs (specifically, sine waves of differing spatial frequencies) and if the output (density distribution) is known for each such elementary input, then the overall output is simply a weighted sum of the elementary outputs. Stationarity means that the system point spread function (i.e., the density distribution resulting from a point exposure source of unit amplitude) has a constant shape at all locations in

the total image area. If both linearity and stationarity obtain, then the system output is simply the input (mathematically) convolved with the point spread function.

The line spread function is the response of a photographic system to a line input and is developed from the point spread function by (mathematical) integration over one spatial dimension. For physical reasons, the line spread function is more amenable to empiric estimation than is the point spread function. Specifically, if an edge is imaged, then the (mathematical) derivative of the edge spread function (i.e., the system's density response to a Heaviside function input exposure distribution) is the line spread function.

The ratio of the output to input modulations, for a sinusoidal exposure, is a function of the spatial frequency (which does not change) and is equal to the modulus of the Fourier transform of the system spread function evaluated at that frequency. This ratio, computed or measured over a range of spatial frequencies, is the MTF.

The MTF of a photographic system is, then, a general descriptor of that system and, further, may be estimated by accomplishing the following steps:

1. Image an edge.
2. Convert the recorded density distribution to an exposure distribution.
3. Differentiate to obtain the line spread function.
4. Fourier transform to obtain the MTF.

This process is shown in Figure 2.

There are advantages and disadvantages to using edge targets in obtaining MTF estimates. The major advantages are that edges occur in the real world, particularly in cultural areas, and that edge images can be recorded as digital density values (for further processing) with relative ease by using a microdensitometer. The disadvantage is that is must be estimated in the presence of emulsion grain noise, and the envelope of the Fourier integral

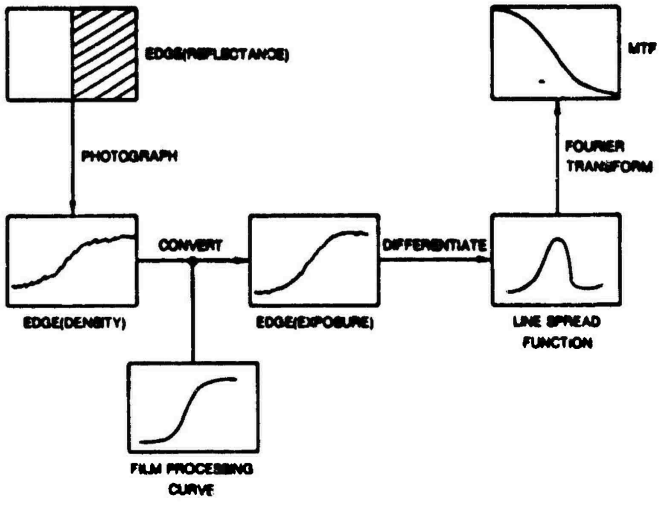

Figure 2. Process to Obtain MTF from Edge Target

of the Heaviside function decreases monotonically with increasing spatial frequency, resulting in a decreased signal-to-noise ratio. A more favorable signal-to-noise ratio is usually attempted by employing a long, narrow slit in the microdensitometer, but this introduces constraints in edge selection and slit/edge alignment.

The application of the MTF to systems design and analysis is of unquestioned utility. From a mathematical point of view, the MTF is a highly tractable describing function. More importantly, perhaps, is the practical consideration that a photographic system can be synthesized from its component parts by the cascading (forming the joint product) of their respective MTFs. It is typical (e.g., Jensen, 1968) to treat the total system response in terms of the products of the MTFs for the lens, film, atmospheric turbulence, and image motion.

The MTF can be applied to the prediction of the system resolving power limit by combining it with a second describing function, the aerial image modulation (AIM) curve. The AIM curve is the threshold (50 percent response) resolving power measure (see above) for a film/processing combination. It is estimated by reading sets of tribar targets impressed on the film at

incremental modulations. AIM curve data are published by film manufacturers. Rodriguez-Torres and Summers (1976) and Fryer (1977) describe laboratory procedures for generating such threshold functions. These curves are overlayed onto the MTF and the intersection is deemed to be the resolution limit. AIM curves are based on an assumed high contrast (1000:1, typically) input to the camera system and must be modified in practice to correspond to the actual contrast presented to the lens. This is accomplished by either multiplying the camera system MTF or dividing the AIM curve by the specific target modulation of interest. Numerous MTF/AIM predictions of limiting resolution appear in the literature. Berkovitz (1969) reported "close correlation" between MTF/AIM predictions and RP estimates and noted that "this correlation indicates that combining the lens MTF with the film modulation detectability curve is an accurate and reliable method of predicting the resolution of a photo-optical system." Sikora and Kuperman (1970) reported on the use of MTF/AIM in determining limiting RP for a reconnaissance system undergoing flight test evaluation. Brock (1967) pointed out the AIM curve is based on tribar (i.e., square wave) targets, while the MTF assumes a sinusoidal input, but stated that "the prediction of resolving power from MTFs and thresholds, though theoretically undefensible, gives useful results and is widely used because of its convenience."

Two different MTF/AIM image analysis programs were utilized during the present research. The first was developed by the Dynamics and Environmental Evaluation Branch of the Air Force Avionics Laboratory (AFAL/RWF). The procedure used is documented in Gliatti (1977) and Kress and Gliatti (1977). The steps are essentially those shown in Figure 2, with the addition of ensemble averaging of multiple microdensitometer scans across an edge to provide "an unbiased estimate of the density profile on the edge and an improvement in the signal-to-noise ratio approximately equal to the square root of the number of scans" (Gliatti, 1977).

The second image analysis was performed by Mead Technology Laboratories, Inc., (MTL) Dayton, Ohio, as a commercial service. Although not explicitly identified as such, AFAL-TR-74-218, "Photographic Systems Performance Analysis Using Double-Annulus Targets," appears to document the procedure

followed in generating the estimates of limiting RP by the MTF/AIM method as used at MTL.

Section 4
RP STUDIES OF IMAGE MOTION

Applied research into quantifying the effects of image motion on camera system RP performance falls naturally into two categories. Uncompensated image motion, introduced by insufficient correction for the angular motion (with respect to the ground scene) caused by the forward movement of the film plane during the exposure period, is common. Image motion compensation (IMC) error is linear in nature and is proportionate to:

$$(V/H)\ (\cos \theta)$$

where

V = ground speed
H = altitude (same units of distance as V), and
θ = (forward) obliquity angle (radians)

Linear image motion effects on RP are covered analytically in Brock (1967) and Rosenau (1963). A detailed description of laboratory measurements is given by Wernicke (1959). A more interesting case of sinusoidal motions and image quality losses is presented by Sun (1967). The present research is, in part, a replication of a portion of Sun's experiments and so his work was of major importance to the author. Sun's method of generating his experimental photography is specified in his report. The method used in the current study is almost identical. (See Section 5, METHOD.) He performed the series of experiments that are summarized below.

Amplitude Effects: The conditions were:

Frequency	= 30 Hz
Amplitude	= 0.00025 through 0.00150 inch
Shutter Speed	= 250 milliseconds
Target	= High, medium, and low (nominal) contrast

The results of this test were that "resolution drops very rapidly in the region from stationary to 0.0005 inch amplitude" and that "for amplitudes larger than 0.001 inch, resolution decreases slowly as vibration amplitude increases." Sun also pointed out "that for vibration amplitudes larger than 0.0005 inch the resolutions obtained with all three degrees of target contrast were very nearly the same."

Target Aspect Ratio: This was a replication of the amplitude effects experiment except that "a high contrast USAF standard target" was used. (The Amplitude Effects experiment employed tribar patterns which exhibited constant bar length and bar widths which decreased according to the sixth-root-of-two; they were thus variable-aspect ratio targets, whereas the USAF 1951-type target maintains a constant 5:1 length-to-width aspect ratio.) Sun found "that the results are essentially the same" and concluded that "this demonstrates that the aspect ratio difference between the two types of target does not produce significant difference in the test results." He based this finding on the subjective comparison of two plots, each of RP versus vibration amplitude, for the two (nominally) high contrast targets.

Frequency Effect: The targets were of high, medium, and low contrast and variable aspect ratio. The vibration amplitude was held constant at 0.00025 inch and the shutter speed at 250 milliseconds. Vibration frequencies were varied over the range 5 through 50 Hz. The result was that "resolution is independent of vibration frequency for fixed amplitude."

Exposure Effect: The Frequency Effect conditions were modified as follows:

Amplitudes:	0.00025, 0.0005, and 0.001 inch
Frequencies:	20 and 40 Hz

and the exposure was varied one-half stop above and below the normal setting through the use of neutral density filters. Sun concluded

"that the variation of exposure in this range has no significant effect on resolution."

Rotation Effects: The conditions were:

Target:	Medium contrast, variable aspect
Shutter Speed:	250 milliseconds
Frequency:	30 Hz
Amplitude:	0.00025 and 0.0005 inch and the target was rotated through several orientations between 45 degrees either side of the normal orientation (i.e., bar widths perpendicular to the direction of the displacement).

Sun concluded, based on a comparison against the medium contrast target RP data from the Amplitude Effects study, that "resolution depends only on the image excursion perpendicular to the target bars," that is, across the width of the bars.

Low Frequency Effect: This was a primarily analytical treatment of the case in which "only part of the vibration cycle is included during the shutter open time." The major effect was found to be due to the image excursion and similar to the linear motion case.

Sun's experiments form the baseline on which the methodology of this present research was developed. The independent variables of his Amplitude Effects and Target Aspect Ratio studies are replicated (as described in the next section). Further, a predictive model, suggested by Sun, is described and applied in Section 6.

Section 5
METHOD

IMAGERY

Since the intent of this study was to compare image quality estimation techniques, the stimulus set was created to provide a broad range of image quality. This was done by imposing sinusoidal image motion (at a constant frequency of 30 cycles per second) during the 1/4-second exposure period. The amplitude (peak-to-peak) of the film plane displacement was varied between 0.0 and 0.00150 inch in increments of 0.00025 inch. A second dimension of image quality variation was introduced through the use of four different target contrasts. A USAF 1951-type target having a nominal density difference (between the light and dark areas) greater than 2.00 and three versions of an "L" target exhibiting nominal density differences of 2.50, 0.90, and 0.20 were used. The imagery set was, then, a 7-levels-of-vibration amplitude by 4-levels-of-target contrast in a full factorial arrangement. Four replicate photographs were present at each of these 28 conditions. Each of the image quality evaluation techniques was applied to all 28 photographic conditions (with the single exception noted below). Figure 3 presents the photographic conditions used in this experiment.

AMPLITUDE OF 30 Hz SINUSOIDAL VIBRATION	USAF 1951	HIGH CONTRAST "L"	MEDIUM CONTRAST "L"	LOW CONTRAST "L"
0.00000(inches)	(4 REPLICATES)			
0.00025				
0.00050				
0.00075				
0.00100				
0.00125				
0.00150				

Figure 3. Design of Imagery Set

DESCRIPTION OF PHOTOGRAPHIC SYSTEM

The controlled production of stimulus materials is crucial to the validity of any image quality assessment research effort. The imagery used in this study was provided by the Dynamics and Environmental Evaluation Branch of the Air Force Avionics Laboratory and was created by following the procedures in Sun (1967). Figure 4 presents a cutaway drawing of the photographic system that produced the stimuli used in this experiment. The main components of the system and the calibration procedures followed are described below.

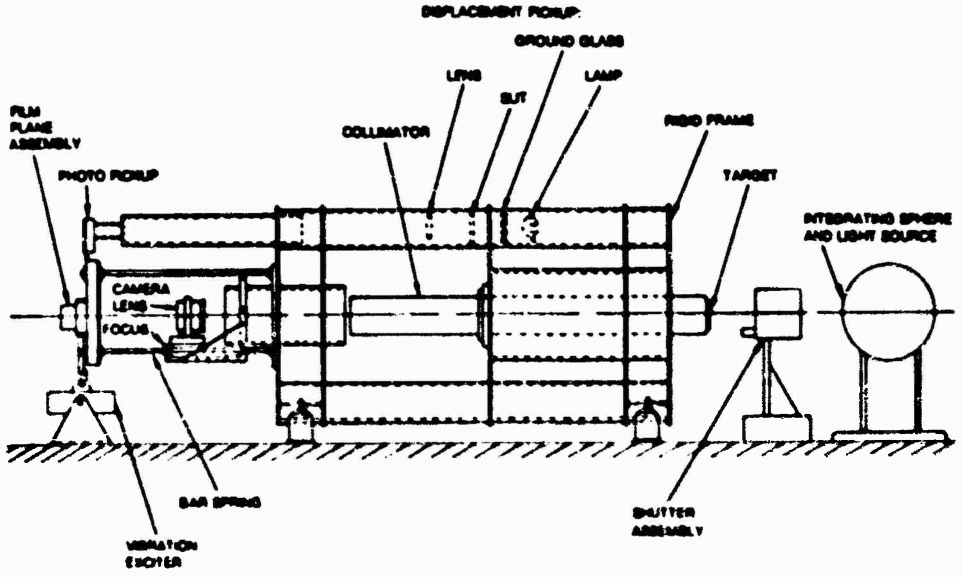

Figure 4. Side Elevation of Photographic System

Light Source

A 400-watt quartz-iodine lamp was used as the source. The lamp yielded a nominal 7500 lumens at a color temperature of 2900 degrees Kelvin. It was mounted at the center of an 18-inch-diameter integrating sphere (painted with five coats of Burch Photometric Sphere Paint No. 2210). An aluminum baffle, also coated with sphere paint, was suspended by fine wires to shield the 2-inch exit pupil of the sphere from direct illumination by the source. The light source was operated at 3.2 amperes.

Shutter Assembly and Shutter Efficiency Test

A 3.5-inch Rapidyne electric shutter was employed to control exposure time. The shutter control unit provided selectable shutter speeds between 1/25 and 1.27 second. The shutter had two sets of leaves, one normally open and one normally closed. Two pulses, generated by the shutter control unit, sequenced the operation of these leaves; the interval between the pulses was the exposure time. At the first pulse, the normally closed leaves sprang open. At the second pulse, the normally open leaves sprang shut. The second pulse also initiated a cam action which reset the leaves for the next shutter operation.

A perfect shutter would be one which was capable of instantaneous opening or closing, (i.e., a rectangular wave response). A real shutter's operation is represented by a trapezoidal response because of the time required for it to reach the full-open or full-closed state. The efficiency of a real shutter is the ratio of the areas of the trapezoid to the rectangle. (The following shutter efficiency test was performed after the collimator and lens were aligned and calibrated.)

The exit of the collimator was partially masked by inserting a glass slide, which had been opaqued except for a small central section, into the target holder of the collimator. (The unmasked region corresponded to the location of the target image during stimulus production.) A Sensor Technology ST-202 photovoltaic semiconductor photosensor was located at the focal plane of the lens in place of the film. The unmasked region of the glass slide was sufficiently small to permit all light to fall on the responsive surface of the photosensor. A Fairchild Model RA741C amplifier was used to amplify the photosensor output for display on either an oscilloscope or chart recorder. The recorded output was compared against an ideal rectangular waveform, following the procedure given in Kuperman (1966), and a planimetric measurement was made for computing shutter efficiency. The measured efficiency was found to be better than 97 percent. Figure 5 presents the waveform comparison used in measuring shutter efficiency.

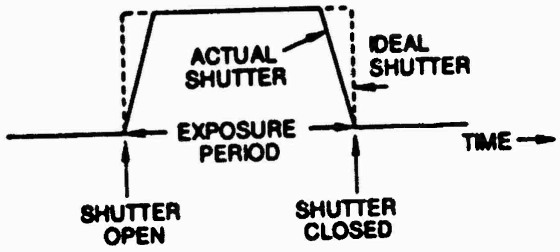

Figure 5. Shutter Efficiency Comparison

Targets

Two types of tribar targets were used in this investigation. The first was a USAF 1951 design (see above), which was a master target (i.e., an original from which other targets may be made by photographic duplication). It was a high contrast target, in a Military Standard 150A sense, with a density difference between the clear bars and dark background greater than 2.00. The three other targets were nonstandard. All were contact exposed from a master Data Corporation "L" target. The "L" target differed spatially from the USAF 1951 target in two ways. First, orthogonal patterns are separated into two legs (as in the 51/51 mobile field test target) rather than being presented adjacent to each other. The second difference is that the length of each bar is constant, which causes the aspect ratio of the bar to increase as the bar width decreases. The aspect ratio of the widest bar was approximately 90:1. Three "L" targets were made photographically from a master target and neutral density filters were interposed during these exposures to achieve different target contrasts. The density differences for the resulting high, medium, and low contrast "L" targets were 2.50, 0.90, and 0.20, respectively. Figures 6 and 7 present the designs of the two types of tribar targets used in this study. It should be noted that both target types provide identical Group/Element (bar width) presentations except that the "L" target has an additional value at the highest resolution (smallest bar width). Both follow sixth-root-of-two progressions.

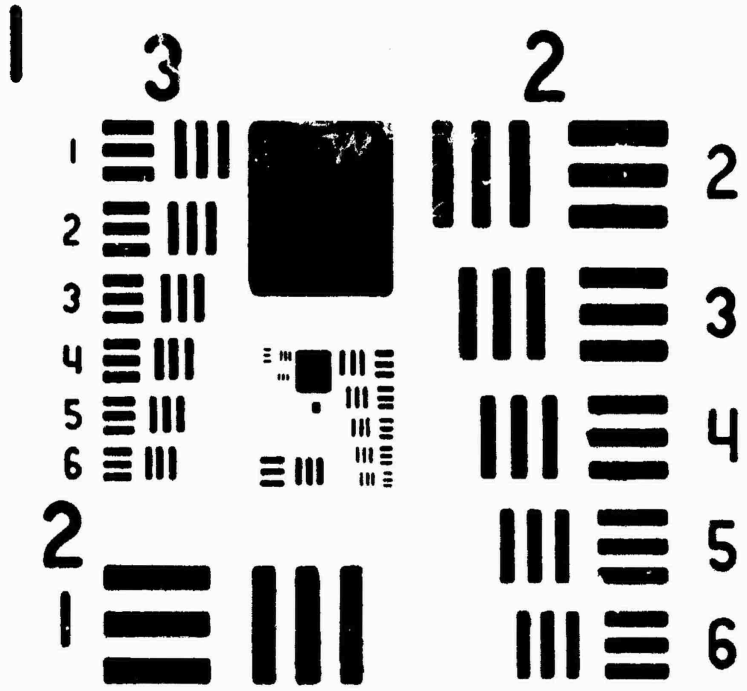

RESOLUTION VALUES

GP-EL	L/MM	GP-EL	L/MM	GP-EL	L MM	GP-EL	L MM	GP-EL	L/MM	GP-EL	L/MM
2-1	4.00	3-1	8.00	4-1	16.0	5-1	32.0	6-1	64.0	7-1	128
2-2	4.49	3-2	8.98	4-2	18.0	5-2	35.9	6-2	71.8	7-2	144
2-3	5.09	3-3	10.1	4-3	20.2	5-3	40.3	6-3	80.6	7-3	161
2-4	5.66	3-4	11.3	4-4	22.6	5-4	45.3	6-4	90.5	7-4	181
2-5	6.35	3-5	12.7	4-5	25.4	5-5	50.8	6-5	102	7-5	203
2-6	7.13	3-6	14.3	4-6	28.5	5-6	57.0	6-6	114	7-6	228

Figure 6. USAF 1951 Target Layout

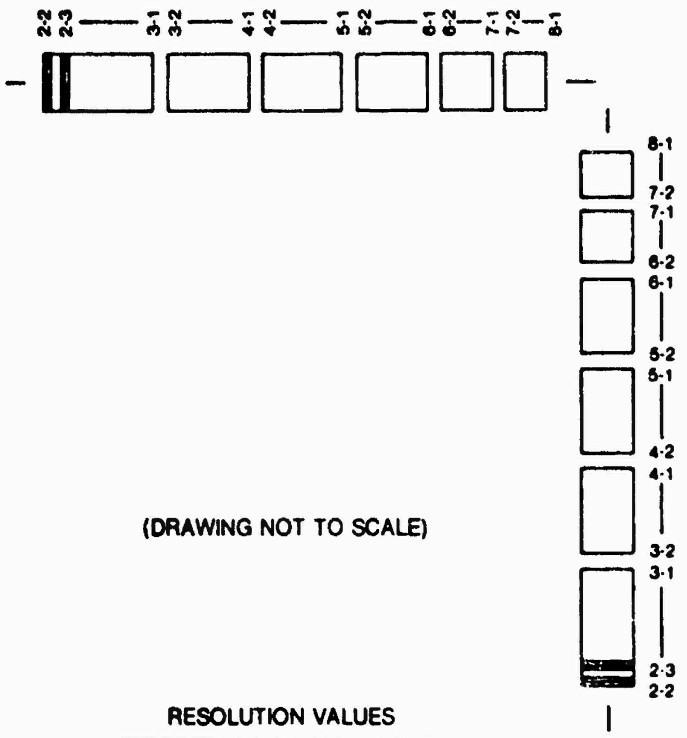

RESOLUTION VALUES
(POSITION AS SHOWN ABOVE)

GP-EL	L/MM	GP-EL	L/MM	GP-EL	L/MM	GP-EL	L/MM	GP-EL	L/MM	GP-EL	L/MM
2-2	4.49	3-2	8.96	4-2	18.0	5-2	35.9	6-2	71.8	7-2	144
2-3	5.09	3-3	10.1	4-3	20.2	5-3	40.3	6-3	80.6	7-3	161
2-4	5.66	3-4	11.3	4-4	22.6	5-4	45.3	6-4	90.5	7-4	181
2-5	6.35	3-5	12.7	4-5	25.4	5-5	50.8	6-5	102	7-5	203
2-6	7.13	3-6	14.3	4-6	28.5	5-6	57.0	6-6	114	7-6	228
3-1	8.00	4-1	16.0	5-1	32.0	6-1	64.0	7-1	128	8-1	256

Figure 7. "L" Bar Target Layout

Collimator

An f/10, 80-inch focal length collimator (manufactured by the American Optical Company) was mounted in a rigid, tubular frame. The frame was located on a heavy concrete seismic block to isolate the optical train from environmental vibrations.

Lens

An f/5.6, 24-inch focal length Pacific Optical aerial camera lens was used. It was installed in an optical clamp on a table which was mounted through a machined way interface to the rigid frame. The ways provide for focusing the lens with respect to the collimator. A laser was used to align the lens and collimator (and all other components of the photographic system). The focal plane of the collimator was determined by autocollimation. The position of the camera lens was then adjusted to bring the target image into sharpest focus on a ground-glass slide installed at the focal plane. The collimator-lens arrangement served to reduce the target optically in direct proportion to the ratio of their focal lengths. In this case, the reduction factor was 3.334.

Film Plane Assembly

A 70mm manually-driven film magazine, equipped with a spring-loaded platen, was modified by the addition of a mechanical frame which arrested the forward travel of the platen, fixing the film plane at a constant position. The magazine was mounted onto a triangular metal frame, which, in turn, was mounted to the collimator support frame by means of three steel bars.

A photosensor and its amplifier, identical to those used with the shutter assembly, were mounted at the top of the film plane assembly. Within the upper tubular section of the collimator support frame, a 100-watt quartz-iodine lamp illuminated a sharp, transmissive edge through a lens to form an image on the photosensor. Vertical movement of the film plane from the rest position resulted in either an increase (upward displacement) or decrease (downward displacement) of the voltage output from the photosensor, as depicted in Figure 8.

Vibratory Excitation

A Hewlett-Packard Model 202A oscillator was used to generate a sinusoidal waveform of the required frequency and amplitude. This signal was fed

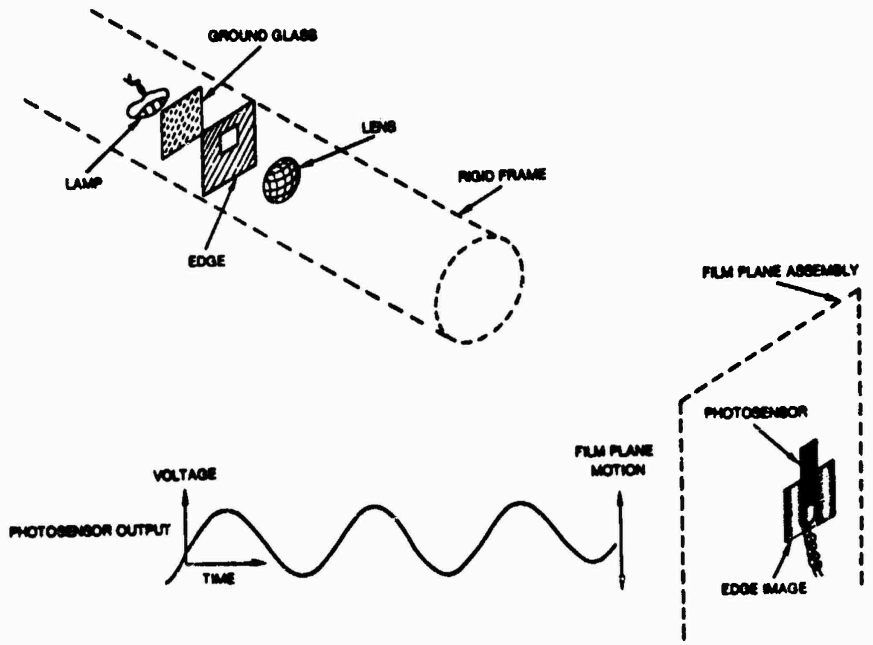

Figure 8. Displacement Pickup System

through a preamplifier (having a feedback circuit for gain control) into a power amplifier which drove an MB Model 531 vibrator, which in turn moved the film plane.

At a given frequency of sinusoidal motion, the dynamic force required to achieve a specific peak-to-peak displacement amplitude is given by:

$$F = M \frac{A}{2} (2\pi f)^2$$

where

F = force (pounds)
A = peak-to-peak amplitude (inches)
f = frequency (cycles/second), and
M = mass of film plane assembly (slugs)

Since the weight of the film plane assembly was 22 pounds, this equation reduced to:

$$F = 1.12\ A\ f^2$$

Since measuring the dynamic force was not a practical means of controlling the film plane motion, the film plane assembly photosensor was calibrated to facilitate control of the displacement. The lamp current was fixed at 6.05 amperes. Weights (corresponding to the dynamic force) were added to the film plane assembly and the resultant displacements were confirmed from a 0.0005-inch-resolution dial gauge. The output voltages were recorded. Figure 9 shows the relationship between displacement of the film plane and pickup photosensor voltage output. The gain of the amplification circuit driving the vibrator was adjusted during photography collection until the voltage from the photosensor matched that corresponding to the required vibration amplitude.

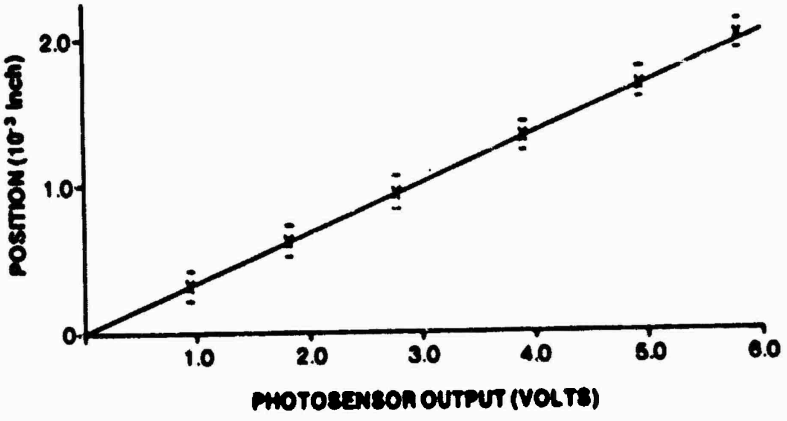

Figure 9. Calibration of Displacement Pickup

Photography

Eastman Kodak Type 3404 high definition aerial film was used. It was processed in an Eastman Kodak black-and-white Versamat at 18 feet per minute,

using one tank and MX-641 chemistry to achieve a gamma of 1.50. The characteristic processing curve is shown in Figure 10.

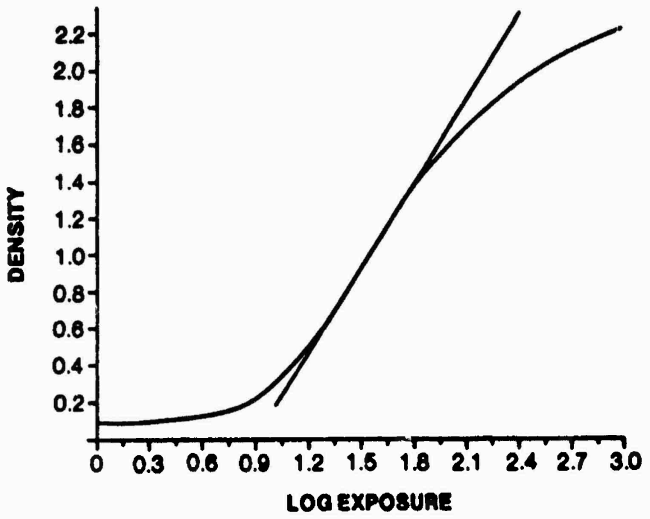

Figure 10. Characteristic Curve for Type 3404 Film

SUBJECTS

All four subjects were males who demonstrated at least 20/20 Snellen acuity (corrected or uncorrected). All were employed in a government laboratory in positions requiring them to perform subjective estimates of photographic image quality as a primary job function. All subjects had received (initial) RP certification (see below) in accordance with the DIA Standard in November 1978. S1 was 24 years of age, had approximately 6 months experience as a reader, and had received graduate level education in Photographic Science. S2 was 41 years old and had 23 years of imagery interpretation experience, almost all of which was in image quality assessment. He had been trained in 1956 as a photographic interpreter. S3 was 38 years of age and had 3 years experience in image quality assessment following completion of a military service correspondence course in photographic interpretation. S4 was 45 years of age and had had exactly the same training and experience as S3. (It is noteworthy that all four subjects were recertified in May 1979 in accordance with the DIA Standard. Thus, criterion performance was demonstrated both before and after the RP readings reported herein were

obtained.) All readers had received on-the-job training in using the VIE technique and had at least 6 months of practical (although intermittent) experience in employing it as a routine part of their assigned duties. Subject S2 had had the most experience, having previously taken part in an in-house investigation of VIE.

RP READER TRAINING AND CERTIFICATION

The DIA Standard requires a four-phase program for the training and certification of RP readers. In Phase I, intended for new readers, the concepts of resolution and test target design are explained (with the Standard serving as the textbook). The criteria for judging whether specific test target elements are resolved are also presented. These are:

A. The image of the bars in the element shall be perceived such that the number of bars could be counted with reasonable confidence even if the number were not known to be three. Otherwise, the element is judged not resolved.

B. Rounding of the corners and shortening of the bars are reasonable effects to expect in a just-resolved test target element. As a guide, the element image should show the three bars as approximately equal in length. However, the element may be judged resolved if any one bar is at least half as long as the other two and the element otherwise meets the criteria of this section.

C. For an element to be judged resolved, there must be a visual perception of density difference between the bars and their surround for the entire length of the bars, even though this density difference may not be uniform for the length of the bar due to grain clumping or other artifacts.

D. A single element that is resolved, but is immediately preceded and followed by elements not resolved, should not be counted. However, if two or more elements are resolved after an unresolved element, then the highest resolved element should be counted.

The artifact of spurious resolution is also introduced and described as "false or misleading [resolution] and is not to be counted as resolved. This false resolution can be described as an image of an element with a phase shift. This characteristic is most often observed as a contrast

reversal in the bar image; i.e., an effective interchanging of the position of bars and spaces. When the shift is present, a different number of lines from the actual number in the target element is observed."

At Phase II, the experienced reader joins the novice in training. This block of instruction is intended to provide motivation; it stresses the need for standard resolution reading rules and procedures. The criterion of reasonable confidence is also developed and motivated. Reasonable confidence "is intended to indicate a level of confidence that is somewhere between complete confidence and no confidence at all." Photographic prints are provided in the Standard to demonstrate both the judgment criteria and the criterion of reasonable confidence. The "school solution" is provided for each example along with a brief comment as to why the given answer is correct (e.g., Criterion D, above).

Phase III concentrates on applied experience. A set of 60 unclassified paper prints of tribar targets is utilized. The trainee practices with subsets of 15 prints, for which he has the answers, until his responses agree (in mean and standard deviation of the reading error) sufficiently with the given values (see the requirement for full certification below).

Phase IV is certification testing. A set of 34 unclassified glass-mounted film chips is employed. "A reader will be deemed fully certified if the mean reading error calculated in both directions is no greater than 6 percent and the standard deviation of the differences is less than 16 percent." (When the author underwent certification training and testing in May 1979, 34 glass-mounted film chips were also used in Phase III instead of the paper prints.) Readers are recertified through the same testing procedure every 6 months.

VIEWING EQUIPMENT

The DoD Standard for tribar assessment is explicit in describing the viewing equipment to be used. This procedure was followed very closely in the present research in collecting both the RP and VIE readings. In the following description of the viewing station, the appropriate sections of the

DIA Standard are presented as direct quotations and the exact configurations used in this research are reported.

> Light Source: "The light source shall be variable and of sufficient intensity. The intensity range shall be such that the luminance of the image seen by the reader can be adjusted to a comfortable level. In general, sufficient intensity means that the maximum available intensity is seldom required and the reader does not feel that additional light would result in improved reading conditions."

The light table used, which includes the light source, was a Richards Corporation Master Interpretation Module System self-standing elevating table equipped with a vacuum stage and Vernac optical-mechanical mensuration feature. The table had been modified to provide a high intensity spot illumination capability. RP and VIE readings were made with the normal light source which has a nominal maximum brightness 2500 footlamberts. None of the readers used the maximum available intensity.

> Microscope: "A variable power, binocular microscope, such as the Bausch and Lomb StereoZoom 7 or equivalent, shall be used to evaluate the imagery."

A Bausch and Lomb StereoZoom 7 power pod was, in fact, used for RP and VIE readings. The eyepieces are inclined 45 degrees from vertical to minimize fatigue. The left eyepiece is equipped for independent focusing (while coarse and fine focus control is provided by raising/lowering the microscope on its overarm carriage). The manufacturer claims resolution of 300 cy/mm (minimum) at a 70X magnification.

> Magnification: "The magnification of the viewing microscope shall be between 0.5 and 1.0 times the resolving power (in cycles per millimeter) that is expected to be read."

The power pod was equipped with 10X, 17mm eye-relief wide-field eyepieces and a 2X supplementary lens attachment. The resulting range of available

magnifications was from 20X through 140X. This range would be appropriate for resolutions in the range from 20 through 280 cy/mm.

> Vibration: "The viewing equipment shall be free of noticeable vibration when viewing imagery at the highest magnification to be employed."

The readers did not report any noticeable vibration nor was any observed by the experimenter. Additional isolation had been achieved through the use of elastomeric isolators between the table and floor.

MICRODENSITOMETRY

All microdensitometry was accomplished on a Mann-Data Micro-Analyzer using a 1 × 60 micron slit aperture. (The procedures for setup and calibration are described in Loosberg, 1972, and Kress and Gliatti, 1977.) One of the target/amplitude photographs was selected for machine reading from each set of four replicates. A single bar, within the largest element, was used to Point Number within that Card/Mark III that he wishes to enter.

The slit width and sample spacing parameters are of most direct importance in any subsequent analysis of the spatial frequency content of the digitized edge, since they determine the spatial frequency cutoff of the microdensitometer. (The modulation transfer function analysis, in particular, requires that these parameters afford sufficient high spatial response to support the reconstruction of the highest spatial frequency recorded by the photographic system under investigation.) The sampling theorem of communication theory requires that, in order to reconstruct a specific spatial frequency, at least two samples must be obtained during a period. This theorem is reflected by the sample spacing. The cutoff frequency imposed by the sampling interval, f_x, is determined as follows:

$$f_x \text{ (cy/mm)} = 1000 \text{ (microns/mm)}/[2 \text{ (samples/cy)} \Delta X \text{ (microns/sample)}]$$

where ΔX is the sampling interval.

The 1-micron sampling interval allows reconstruction of spatial frequencies up to 500 cy/mm. The second parameter, aperture size, is treated similarly. Only the dimension in the scanning direction need be considered. (The slit length permits achieving a more favorable signal/noise ratio by permitting samples to be integrated over a larger area.) The aperture response for the 1-micron slit width is greater than 50 percent at 500 cy/mm.

Thus, the combined sampling and aperture spatial frequency response capability is more than twice the maximum limiting resolution to be expected, based on the lens/film combination (as predicted by the ISL and MTF methods in Section 6).

The maximum amplitude (peak-to-peak) of the induced sinusoidal motion is .00150 inches. A total of 128 samples was recorded on each microdensitometer trace, yielding a scan length of 128 mirrons. The scan length is more than three times the extent of the largest induced motion.

MODULATION

Modulation values for each photograph were derived from the microdensitometer scans. Minimum and maximum density values were found which corresponded to the bar and space, respectively. These were converted to relative exposure space by passing them back through the characteristic film processing curve (Figure 10). Modulation was then computed as the ratio of the sum of these minimum and maximum exposures to their difference. Figure 11 presents the modulation for all 28 conditions. The modulations for the static conditions were:

Target	Modulation
USAF 1951	0.76
High Contrast "L"	0.66
Medium Contrast "L"	0.52
Low Contrast "L"	0.08

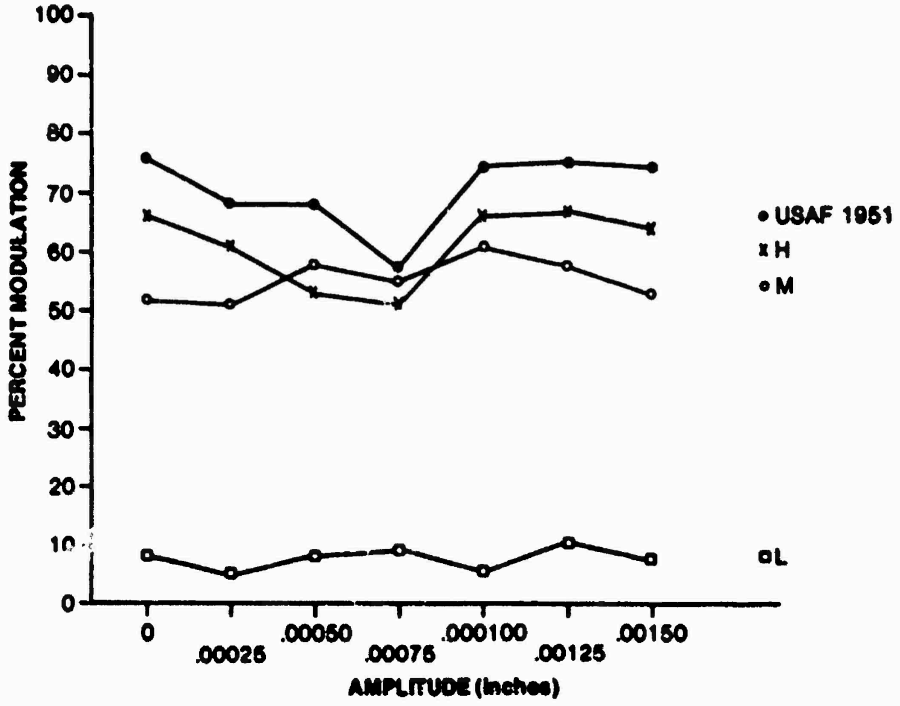

Figure 11. Target Modulation Values

Section 6
RESULTS

PREDICTIVE

In order to develop a model of a system, in this case photographic performance in the presence of sinusoidal image motion, it is usual to apply analytic representations of that process to the a priori information and predict the effects of the process under those conditions. In this research, two such modeling approaches were attempted. The two models are the Inverse Square Law (ISL) and the MTF. Both allow separation of system components into lens, film, and image motion limits, and also support performing a synthesis of these components to predict total system performance in terms of the resulting image quality. (Note: Image quality is considered only in the direction of the applied motion, i.e., the vertical direction in Figure 4.)

Inverse Square Law

The ISL is an extension of a procedure, the reciprocal formula, which provides a simple approximation method. Katz (1963) developed a heuristic rationale for this representation:

> Consider an infinitely narrow line in real space being imaged by a real lens with its limitations. The lens would take this long, infinitely thin line, and spread it out (in the aerial image) to a width W_l; that is, the image width due to the lens itself. Similarly, consider an infinitely narrow line produced by a nonexistent perfect lens and imaged on the film. The film, having a resolution limit all its own, would take this infinitely narrow line and spread it out to a line width W_f (just before it hits the film); the film, receiving this image, would perform its spreading on each edge, making a total of $W_f + W_l$. (This is easily recognized as simple addition of spot size diameters.) But this is not very scientific. I simply introduced the convention that $W_f = 1/R_f$ and $W_l = 1/R_l$, converting widths to resolution numbers, thus producing the ancient formula $1/R_{f+l} = 1/R_f + 1/R_l$.

The resolution limit imposed by image motion is represented by a similar term, R_m. The simple formula was modified to the following form, the ISL:

$$1/R_s^2 = 1/R_\ell^2 + 1/R_f^2 + 1/R_m^2$$

where

R_s = resolution limit of total system (cy/mm)
R_ℓ = resolution limit of lens (cy/mm)
R_f = resolution limit of film (cy/mm)
R_m = resolution limit due to image motion (cy/mm)

(Wernick, 1959, for example, used both forms.)

Using the ISL, we can predict the results of the experiment by computing the resolution limit of each component and taking square root of the reciprocal sum of the squares of the individual limiting resolutions.

R_ℓ: Assuming a diffraction limited lens and applying the Rayleigh criterion for resolution, we have:

$$R_\ell = \frac{D}{1.22\ \lambda\ F} = \frac{1}{1.22\ \lambda\ f}\ \text{(cy/mm)}$$

where

D = lens diameter (4.29 inches)
F = lens focal length (24 inches)
f = relative aperture (f/5.6), and
λ = effective wavelength of white light (5.55×10^{-4}/mm)

We obtain

R_ℓ = 264 cy/mm

R_f: Manufacturer's published film limiting resolution data for Type 3404 film is available for two input contrast ratios, C_i = 1000 and C_i = 1.6 (where C_i is the ratio of the maximum illumination from the target to the minimum).

Since the film resolution limit is dependent on the input target modulation, a computational method (Fraggiotti, 1979) can be employed to find R_f at the modulations of interest (0.76, 0.66, 0.52, and 0.08; see Section 5).

The published resolution limits are based on the MTF and the Threshold of Detectability (TOD) curves shown in Figure 12. (The MTF for Type 3412 film, a newer high resolution aerial reconnaissance material, is also shown for comparison.) The MTF curve is from the Eastman-Kodak Data Sheet for high definition aerial film Type 3404. The TOD curve is made up of two segments. The low spatial frequency portion (out to about 25 cy/mm) represents the modulation required by the observer to report the presence (detect) of a pattern 50 percent of the time. Various values between 2 and 4 percent modulation have been reported and a value of 3 percent is used in the figure (RCA, 1974).

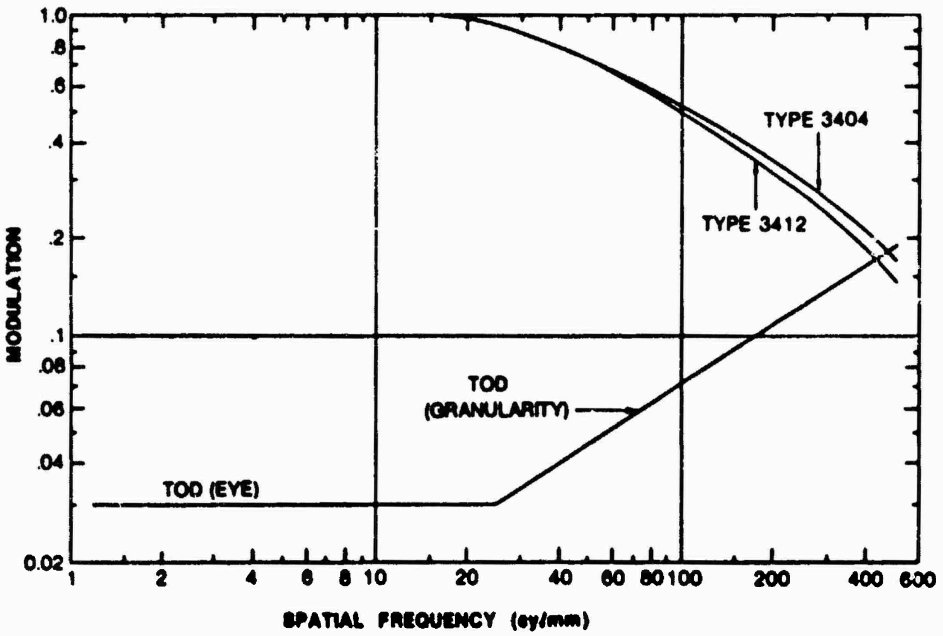

Figure 12. MTF for Type 3404 and 3412 Photographic Emulsions

The high spatial frequency portion of the TOD curve is based on film granularity. Granularity is defined as the subjective impression caused by the film grain distribution. Selwyn (1935) proposed the following formula to represent granularity data:

$$G = \sigma_d \, (2\,A)^{1/2}$$

where

G = granularity
σ_d = standard deviation in density about a mean value
A = area of scanning aperture

Kodak measures granularity at a density of 1.0 above base plus fog, using a spot aperture of 48 microns diameter. The published diffuse granularity for Type 3404 film is 9.7. The portion of the TOD curve in Figure 12 due to granularity is from Coltman (1954). The limiting resolutions for the film at the required modulations were found by shifting the MTF curves down (as shown in Figure 13) and reading their intercepts with the TOD curve. (The 1000:1 contrast MTF curve $M_i(5)$ is retained for reference.)

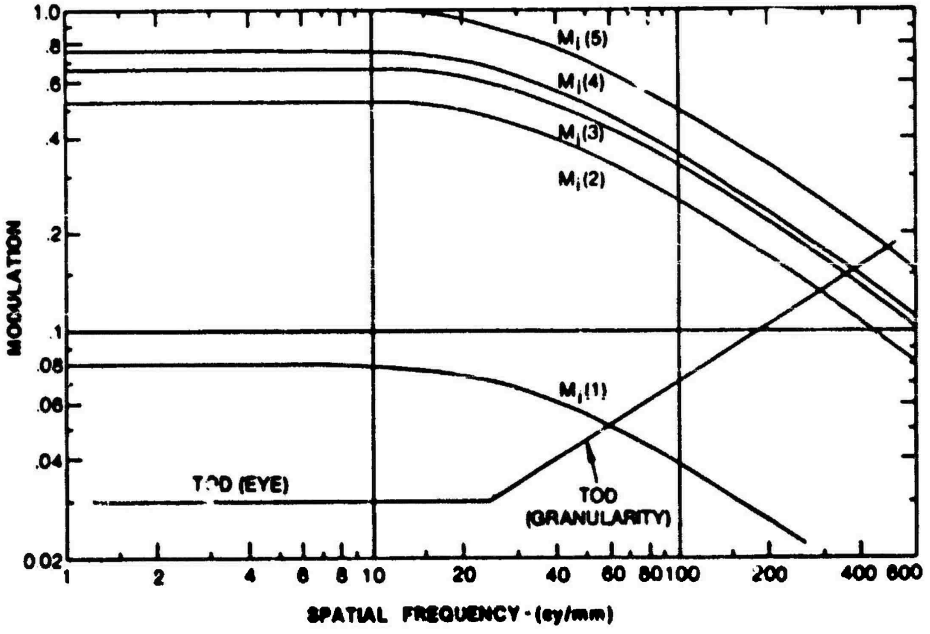

Figure 13. Limiting Resolution of Type 3404 Emulsion for Several Contrasts

The following film limiting resolutions were found for the four modulations of interest:

Modulation		Limiting Resolution (cy/mm)
$M_i(5)$	1.00	475
$M_i(4)$	0.76	370
$M_i(3)$	0.66	345
$M_i(2)$	0.52	290
$M_i(1)$	0.08	58

R_m: The limiting resolution due to sinusoidal image motion is given by the equation:

$$R_m = 1/a$$

where

a is the peak-to-peak amplitude (in mm)

The values of R_m, then, depend only on a and, in the present experiment, were found to be:

a (inches)	R_m (cy/mm)
0.00000	∞
0.00025	157.5
0.00050	78.7
0.00075	52.5
0.00100	39.4
0.00125	31.5
0.00150	26.2

The ISL was then used to combine the R_ℓ, R_f, and R_m values to find the R_s values for each to the 28 conditions of the experiment as shown in Table 1.

TABLE 1. ISL PREDICTED RP VALUES

Peak-to-Peak Amplitude (inches)	Target: USAF 1951 (M_i = 0.76)	High Contrast "L" (M_i = 0.66)	Medium Contrast "L" (M_i = 0.52)	Low Contrast "L" (M_i = 0.08)
0.00000 (static)	215	210	195	56.6
0.00025	127	126	123	53.3
0.00050	73.9	73.7	73	46
0.00075	51	50.7	50.6	38.5
0.00100	38.8	38.7	38.6	32.3
0.00125	31.2	31.2	31.1	27.5
0.00150	26	26	26	23.8

These values are also plotted in Figure 14. From the table and figure, it can be seen that

- the effect of target modulation is pronounced only for the low contrast "L" target and only out to about the 0.00075 inch amplitude condition.

- the effect of image motion is most strongly evidenced out to the 0.00050 inch amplitude condition.

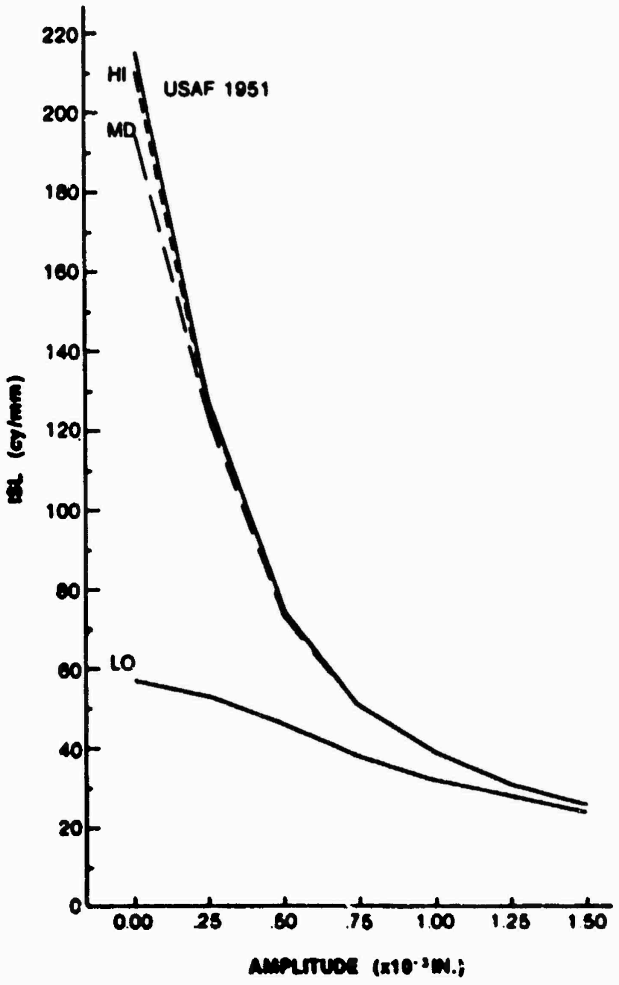

Figure 14. Limiting Resolutions Predicted by ISL Method

MTF

The MTF was described above (Section 3) in the context of image quality analysis. It can also be applied as a predictive tool because the MTF of a system is the product of the MTFs of its components. Modulation M is defined as:

$$M = \frac{I_{max} - I_{min}}{I_{max} + I_{min}}$$

where I_{max} and I_{min} are the (respective) maximum and minimum light intensities. The MTF, T(K), then is the ratio of the output modulation $M_o(K)$ to the input modulation $M_i(K)$ at the spatial frequency K. Because of the multiplicative (cascading) property of the MTF, we have:

$$T_s(K) = T_L(K)\ T_F(K)\ T_M(K)$$

where

$T_s(K)$ = MTF of total system
$T_L(K)$ = MTF of the lens
$T_F(K)$ = MTF of the film
$T_M(K)$ = MTF of the image motion

Although this representation is correct only for a sinusoidally distributed input modulation (at spatial frequency K), the approach can be applied over a range of spatial frequencies for all components and then the TOD curve (defined and described above) can be overlayed to predict limiting resolution for the total system in cycles per millimeter. The following development of components MTFs is adapted from Fraggiotti (1979).

$T_L(K)$: The modulation transfer function for a diffraction limited lens with a clear, circular aperture is given by:

$$T_L(K) = \frac{2}{\pi}\left\{\cos^{-1} bk - bk\left[1-(bk)^2\right]^{1/2}\right\}$$

where

b = the reciprocal of the limiting spatial frequency (mm/cy), and
K = spatial frequency in image plane (cy/mm).

The limiting spatial frequency, K_{limit}, can be found by:

$$K_{limit} = \frac{D}{\lambda F} = \frac{1}{\lambda f} = 322 \text{ cy/mm}$$

where λ, D, F, and f are as above. This formula differs from that used to compute R_L in that the constant 1.22, required by the Rayleigh point separation criterion, is omitted from the denominator. $T_L(K)$ is plotted in Figure 15.

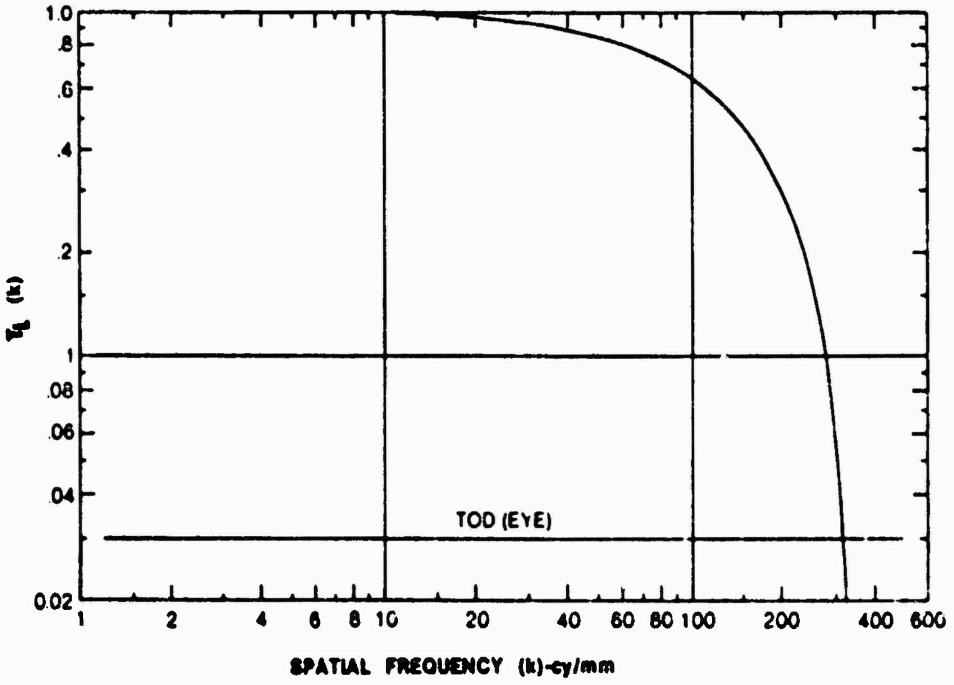

Figure 15. MTF for 610 MM Focal Length Lens

The TOD curve representing only the observer modulation requirement is overlaid on $T_L(K)$. Their intercept is in close agreement with the computed limiting spatial frequency.

$T_F(K)$: The MTF was presented in Figure 12.

$T_M(K)$: Rosenau (1963) discussed the transfer functions for linear, parabolic, random, and sinusiodal image motion. For sinusoidal motion,

$$T_M(K) = J_o (\pi a K)$$

where

J_o = zero-order Bessel Function
a = peak-to-peak amplitude of image motion
K = spatial frequency (cy/mm)

Figure 16 presents $T_M(K)$ for the six amplitudes a(i) used in this experiment.

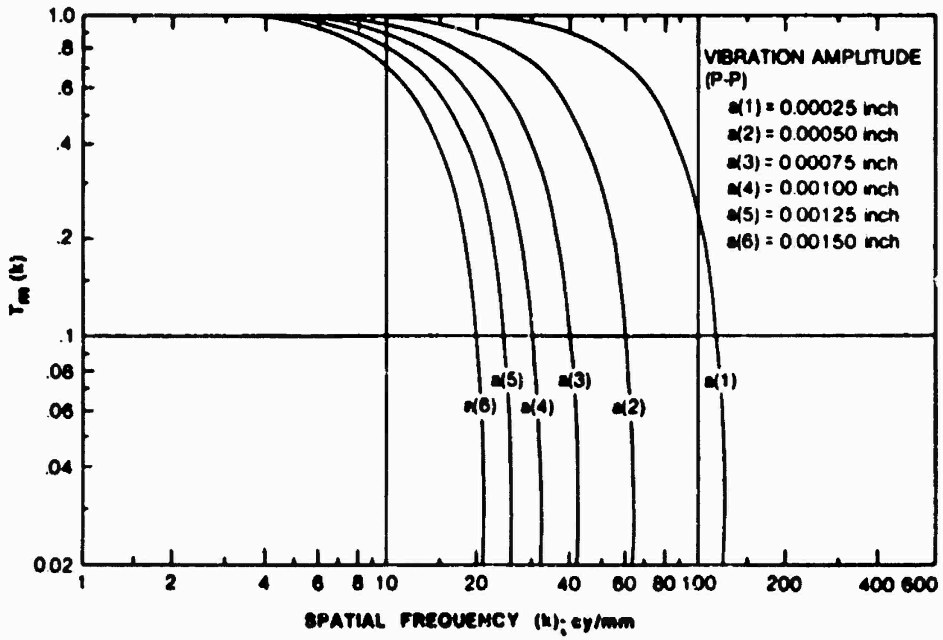

Figure 16. MTF for Sinusoidal Image Motion (Vibration)

$T_S(K)$: The system MTF is the product of the lens, film, and motion transfer functions. Since we have four target modulations and seven vibration amplitudes, (including the static case) there are actually 28 $T_S(K)$ curves to consider. Figure 17 (a through g) presents the system MTFs. Overlaid on each is the TOD curve (now including film granularity). Table 2 summarizes the limiting resolutions predicted by the MTF/TOD intercepts and Figure 18 shows them graphically.

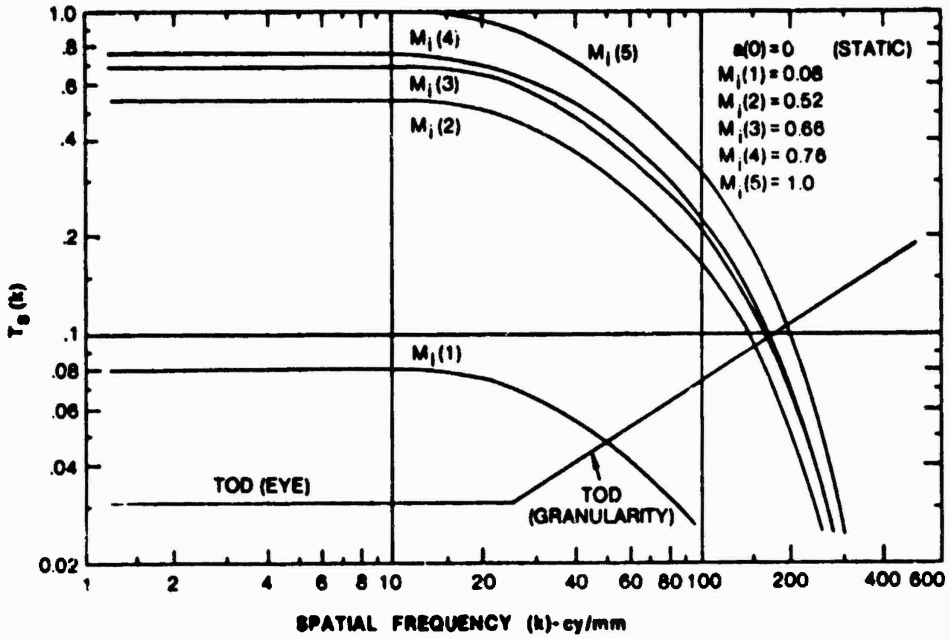

Figure 17a. Composite MTF for Lens, Film, and Vibration Amplitude a(0)

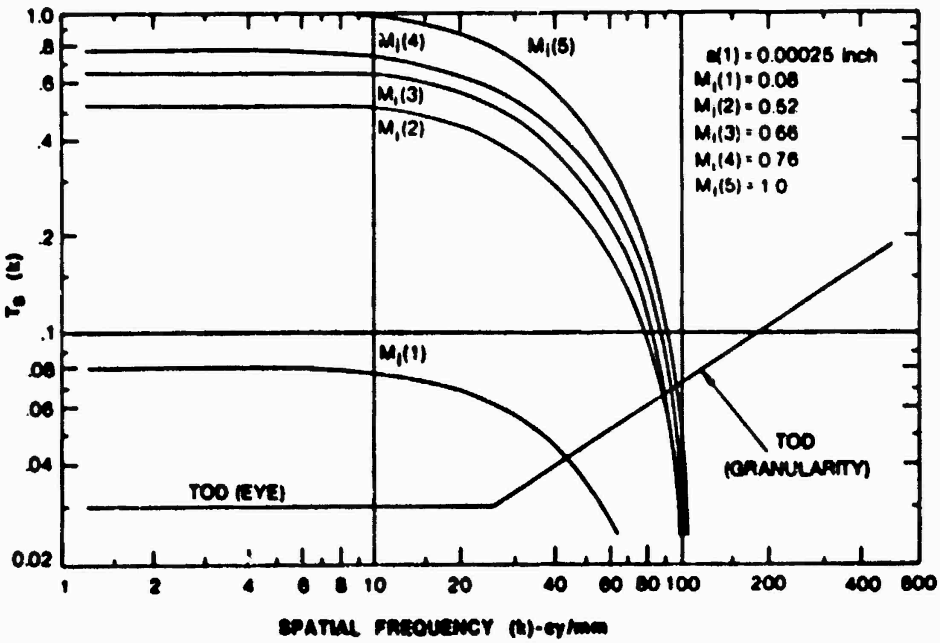

Figure 17b. Composite MTF for Lens, Film, and Vibration Amplitude a(1)

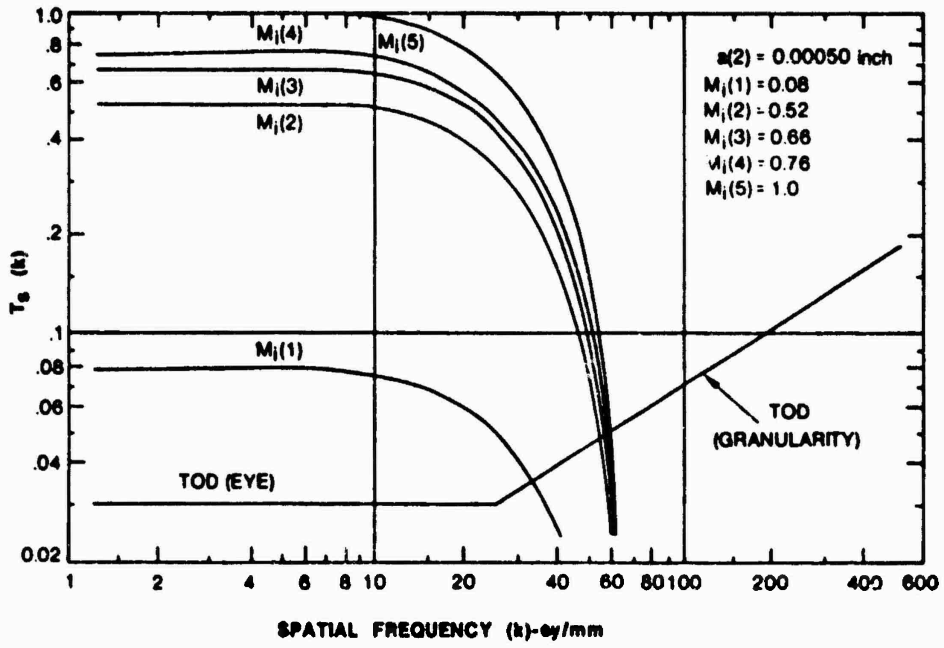

Figure 17c. Composite MTF for Lens, Film, and Vibration Amplitude a(2)

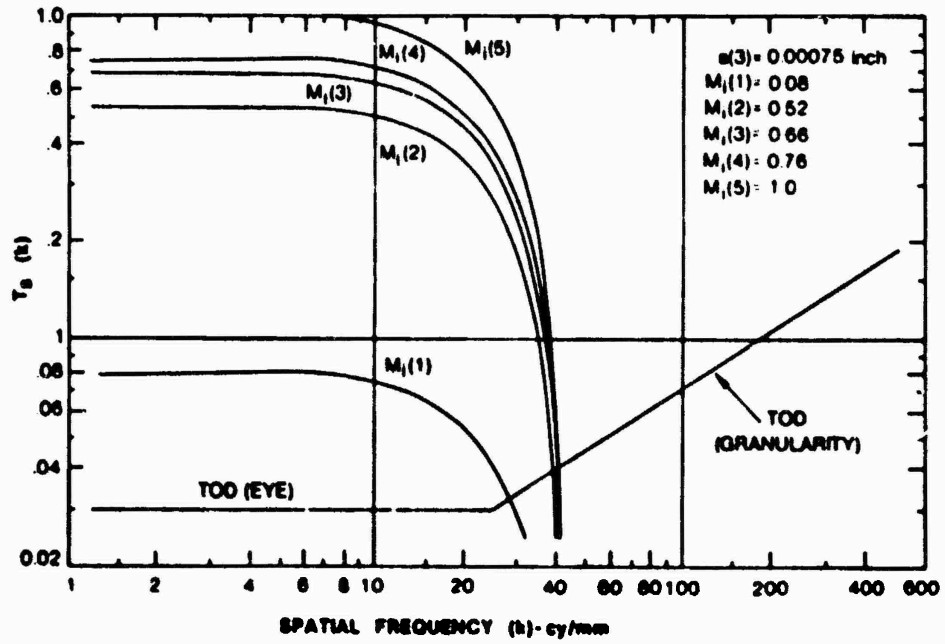

Figure 17d. Composite MTF for Lens, Film, and Vibration Amplitude a(3)

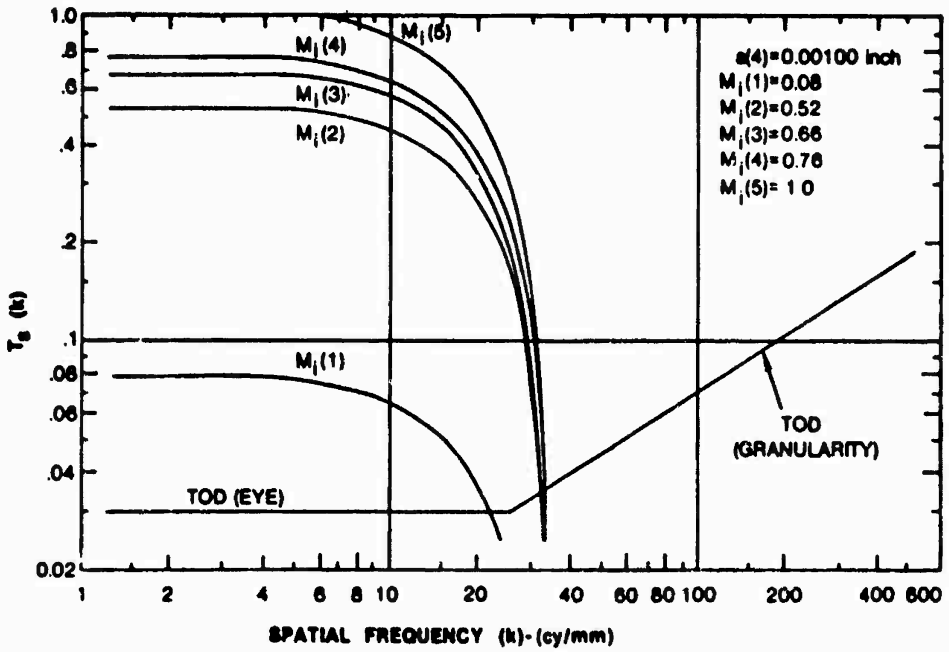

Figure 17e. Composite MTF for Lens, Film, and Vibration Amplitude a(4)

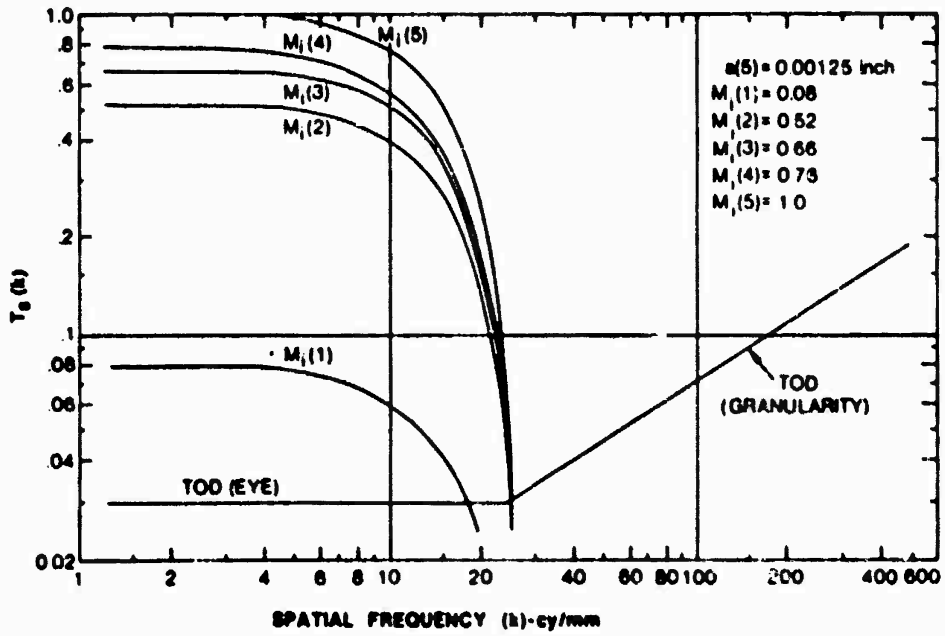

Figure 17f. Composite MTF for Lens, Film, and Vibration Amplitude a(5)

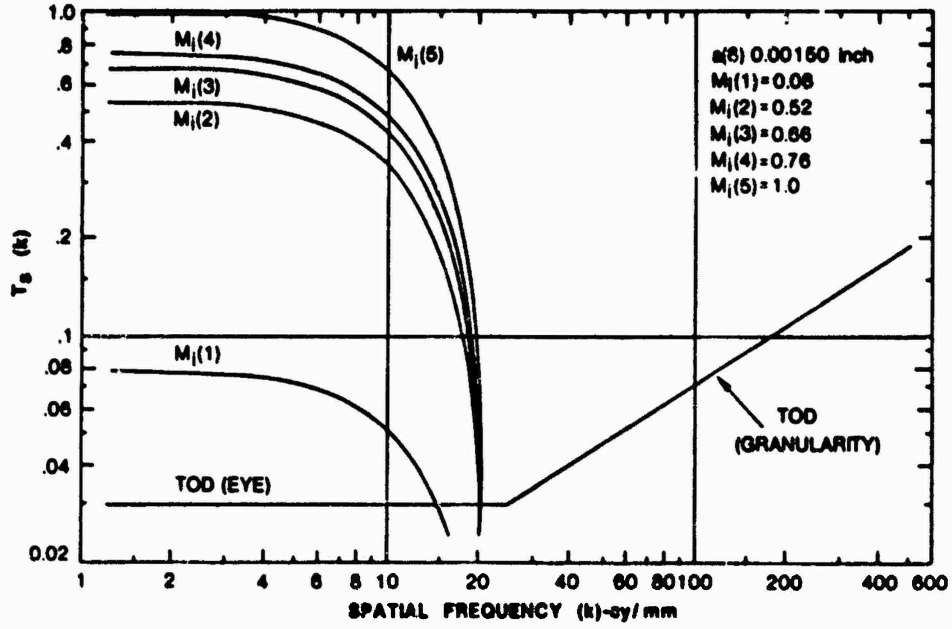

Figure 17g. Composite MTF for Lens, Film, and Vibration Amplitude a(6)

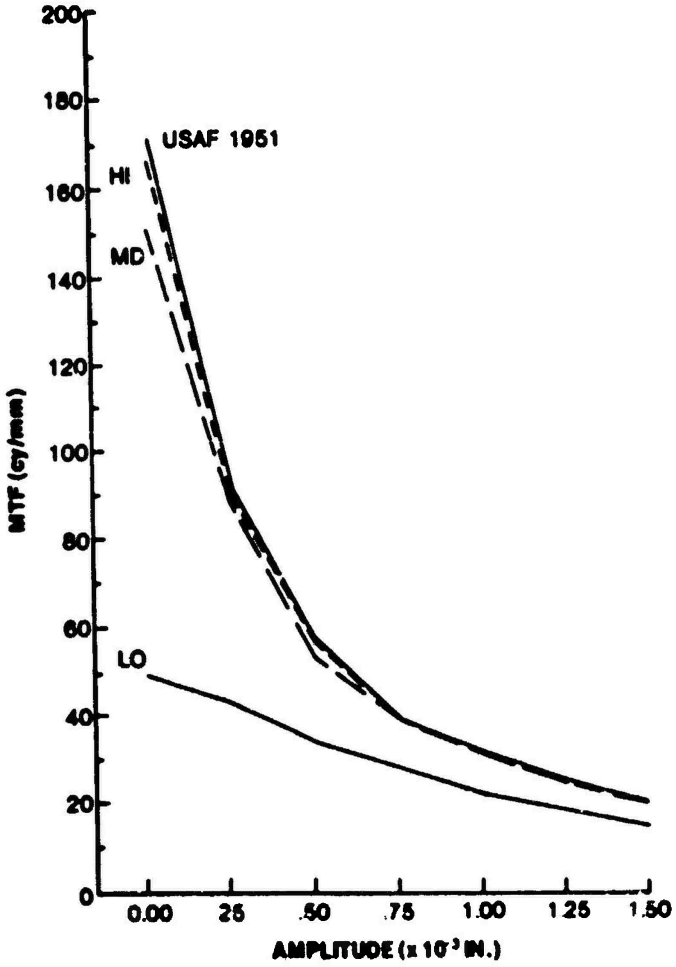

Figure 18. Limiting Resolutions Predicted by MTF Method

TABLE 2. :ITF PREDICTED RP VALUES

Peak-to-Peak Amplitude a(i) (inches)	Target: USAF 1951 (M_i = 0.76)	Target: High Contrast "L" (M_i = 0.66)	Target: Medium Contrast "L" (M_i = 0.52)	Target: Low Contrast "L" (M_j = 0.08)
0.00000	170	165	150	49
0.00025	92	90	88	43
0.00050	57	56	53	33.5
0.00075	39	39	38.7	27.7
0.00100	31.5	31	31	21.8
0.00125	24.6	24.6	24.5	18.5
0.00150	19.9	19.9	19.8	14.8

The same observations made regarding the ISL predictions also hold for those produced by this method.

Comparison of ISL and MTF Predictions:

A regression analysis (BMD03R, Dixon, 1977) was applied to the two sets of predictive data. The two predictors were highly linear in their relationship, yielding a correlation coefficient r = 0.998. The regression equation was found to be:

$$ISL = 1.29\ (MTF) + 1.3$$

The two predictors are in very close agreement over the conditions of interest with the ISL producing somewhat higher values. This difference is probably due, at least in part, to the contribution to limiting resolution imposed by the image motion computation, with the ISL method yielding higher values than the MTF approach. (Compare Figures 14 and 18.)

SUBJECTIVE

RP and VIE measurements were made on the controlled photography using the procedures and criterion described above in Section 2. Additionally, a modified form of the ISL was employed using the static RP readings to initialize the model.

RP

Figure 19 presents the observed RP values for the 28 experimental conditions. The means (four subjects and four replications) are plotted and the error bars show plus/minus one standard deviation.

The major trend shown in the figure is very similiar to that observed in the predictive data from the MTF and ISL models (Figures 14 and 18) in that there is a rapid decrease in RP with increasing amplitude out to the 0.00050 inch condition.

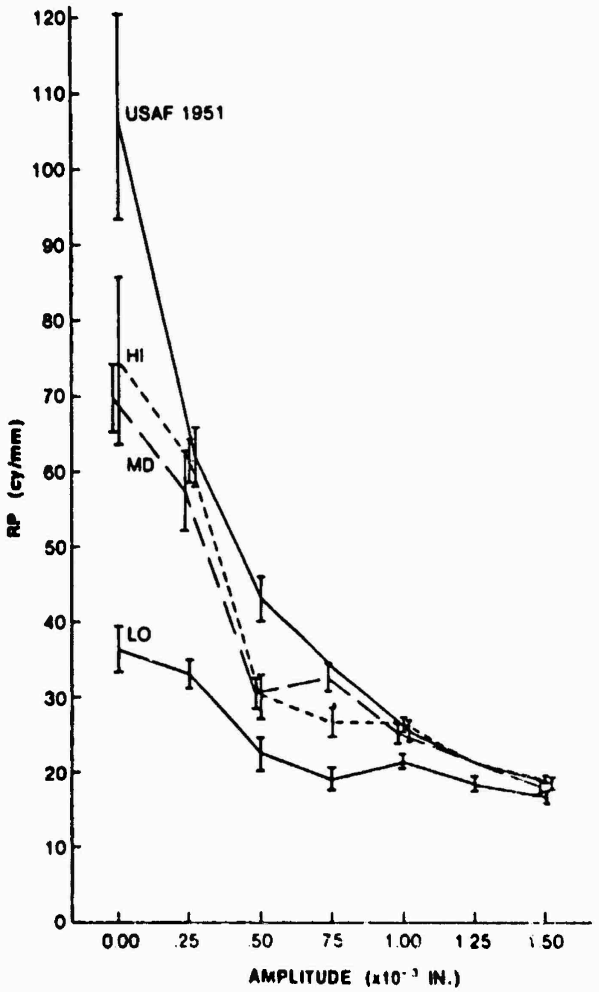

Figure 19. Observed RP Readings

An analysis of variance for a within-subjects, repeated measures design (BNDO8V, Dixon, 1977) was applied to the raw RP data. The results are presented in Table 3.

TABLE 3. ANALYSIS OF VARIANCE: RP

Source	Sums of Squares	df	Mean Square	F	Significance
Subjects (S)	10.59397	3	3.531323	2.432	
Targets (T)	2185.218	3	728.4060	579.831	**
Amplitude (A)	13624.78	6	2270.797	1039.522	**
S × T	11.30615	9	1.256239	.86505	
S × A	39.32031	18	2.184462	1.50422	
T × A	2783.703	18	154.6502	99.53083	**
S × T × A	83.90479	54	1.553792		
Within Repetitions	487.9453	336	1.452218		

* $p \leq .05$

** $p \leq .01$

Three sources of highly significant ($p < 0.01$) effects were identified: Targets, Amplitudes, and the Target × Amplitude interaction.

An Omega-squared post hoc test (Simons, 1971) was applied to determine the percentage of the total variance that was accounted for by each source. (The Omega-squared test is considered to be conservative in that it permits generalizing the results beyond the specific subjects used in the study to the total population.) The results are shown in Table 4. The results of this test were extremely encouraging to the continued use of RP as an image quality estimation technique. The independent variables and their interactions accounted for more than 96 percent of the total variance, with Targets (modulation), Amplitudes (peak-to-peak extent of the sinusoidal motion), and their interaction combining to account for almost all the variance. Conversely, the fact that Subjects accounted for less than one-tenth of one percent of the total variance argues strongly as to the sufficiency of the training and certification procedure in providing stable estimations of photographic system performance.

TABLE 4. OMEGA-SQUARED TEST: RP

Source	Percent of Total Variance Accounted for
Targets (T)	11.3
Subjects (S)	0.03
Amplitudes (A)	70.8
T × A	14.3
T × S	0.00
S × A	0.07
T × S × A	0.03
Total	96.54

The factors and interaction for which significant findings were obtained merit attention. An additional post hoc analysis, Tukey's HSD (honestly significant difference) was applied (Roscoe, 1975). Although targets were

highly s' 'cant, it was found that the high and medium contrast "L" targets were statistically indistinguishable, with USAF 1951 and low contrast "L" being highly significantly different ($p < 0.01$) from the high and medium and from each other.

This was not surprising since, although their nominal contrasts were different, their modulations as measured (see Figure 11 and its accompanying list of measured values) evidenced crossover at the 0.00050 and 0.00075 inch amplitudes conditions. The USAF 1951 and the low contrast targets were different from the other two and from each other (all $p < 0.01$). All the amplitude conditions were significantly different from each other at $p < 0.01$, with the exception of the 0.00075 and 0.00100 inch comparison which was significantly distinct at $p < 0.05$. The Target × Amplitude interaction generally reflected the covarying decrease in RP with decreasing target modulation and increasing vibration amplitude. (See the Appendix for further analyses of the RP data with the high and medium contrast conditions pooled together.)

Comparison of RP to ISL and MTF Values

Because of its longevity and ubiquity in application as an image quality estimation technique, RP was selected to serve as the baseline against which the other estimation methods could be compared. It was of some interest, then, to compare the empiric RP values against the limiting resolutions predicted by the ISL and MTF models.

Figure 20 presents a graphical representation of the three data sets. In constructing the figure, the RP data were collapsed across Subjects and Replications to yield 28 mean observations (4 Targets × 7 Amplitudes). The mean RP data were then ordered in decreasing sequence. The corresponding ISL and MTF predictions were ordered according to the RP data. Subjective inspection of the figure shows generally good agreement between the three curves. Regression analyses (BMD03R, Dixon, 1977) were performed for ISL and MTF predictions with respect to the 28 mean RP observations. For ISL, the correlation coefficient was found to be $r = 0.96$ and the regression equation was

ISL = 2.50 (RP) - 19.2

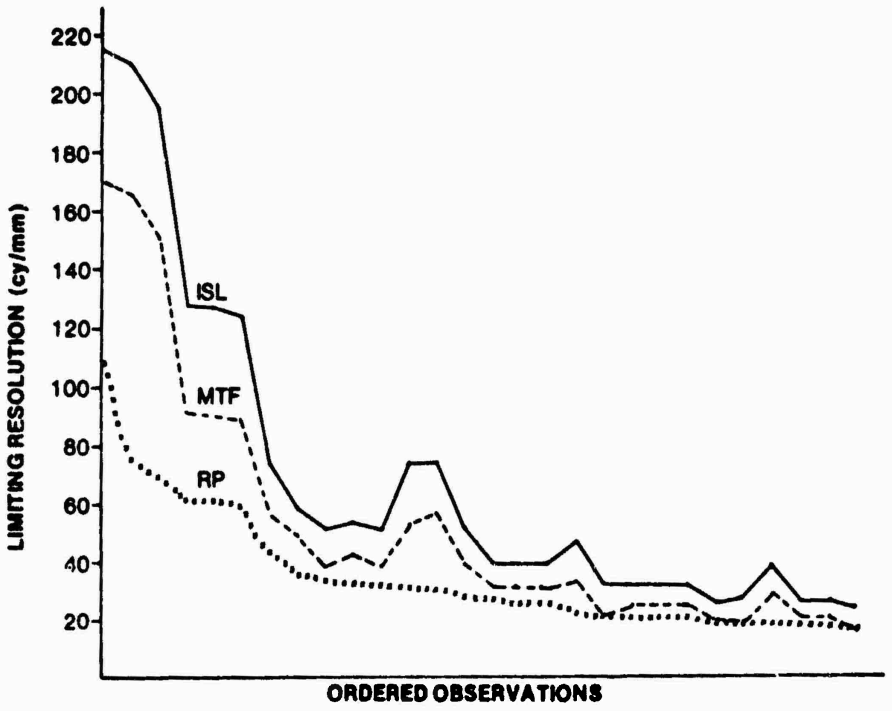

Figure 20. MTF and ISL Predictions vs. Observed RP Values

For MTF, the correlation coefficient was r = 0.96 and the regression equation was

MTF = 1.94 (RP) - 15.78

One explanation of the very high linearities and large slopes (of the regression equations) is the possibility that the DIA criterion for reading RP targets yields consistent and conservative estimates. (The mean RP data will be used as the baseline against which to compare the other empiric image quality estimators.)

Correction for Target Modulation

Mayo, in his 1968 thesis, proposed a formula for correcting RP data on the basis of the target modulation. Based on a survey of published lens/film RP tests, he found "that the variation of photographic resolving power with modulation for aerial reconnaissance lenses typically follows the relationship:

$$R = R_o M^{1/2}$$

His work was optimized for modulations between 0.40 and 0.10. He also pointed out that "these relationships could probably be extended to include such factors as defocus, exposure latitude, image motion, or other lens and film properties." An unsuccessful attempt was made to apply his correction formula to the RP data reported herein. The formula was applied to each of the high, medium and low contrast Target × Amplitude combinations using the USAF 1951 target at that condition as the reference.

After applying Mayo's formula, only the slightest improvement in agreement was found for the high and medium contrast target RP data, while much worse agreement (overcorrection) was found for the low contrast target case. Since the observed average modulation for the low contrast target photography was only 0.08, perhaps this case fell too far out from the usable range of the correction formula. Although the correction was applied separately at each Amplitude level, perhaps an additional extension of the formula is required to correct for image motion of the type used in this study.

Sun Predictive Model

In the similar 1967 experiment, Sun developed a modification of the Inverse Square Law relationship which employed static resolution to account for lens/film performance and a modified analytic derivation of the motion-imposed resolution limit (R_m). He assumed that a bar pattern would not be resolved (limiting resolving power) when "the exposure of the high density and low density areas of the target image become equal due to vibration." He found this condition to occur when:

$$\frac{a}{A} = 1.4$$

where

a = the peak-to-peak amplitude of the sinusoidal motion, and
A = the acceleration

Thus, R_m occurs when

$$\frac{1}{2A} = \frac{0.7}{a}$$

He modified this expression for motion-limited performance, as follows:

$$R_m = C_1 \, C_2 \, \frac{0.7}{a}$$

where "C_1 is a factor for possible human error" and "C_2 is a factor to take care of the film response under image motion." He proposed values of $C_1 = 0.90$ and $C_2 = 0.85$. (Sun pointed out that the adjustment factors C_1 and C_2 were "subject to further theoretical justification" but found that by employing them he achieved predictions which agreed "reasonably well" with his experimental data.) Sun recommended the use of the following equation for predicting the limiting resolution of imagery whose exposure included the presence of sinusoidal vibration:

$$\frac{1}{R_s^2} = \frac{1}{R_o^2} + \frac{1}{\left(\frac{0.535}{a}\right)^2}$$

where

R_s = system (lens/film/motion) resolution (cy/mm)
R_o = static resolution (cy/mm), and
a = peak-to-peak amplitude (millimeters)

From Sun's equation, we expect R_m to take on the following values for the six amplitudes of sinusoidal motion applied in the present study:

a (inches)	R_m (cy/mm)
0.00025	84.3
0.00050	42.1
0.00075	28.1
0.00100	21.1
0.00125	16.9
0.00150	14.0

Then for the four targets in the present study, the total system resolution (R_s) would be predicted to be:

Amplitude (inches)	USAF 1951	High Contrast	Medium Contrast	Low Contrast
static	106.7	74.7	69.3	36.3
0.00025	66.1	55.9	53.5	33.3
0.00050	39.2	36.7	36.0	27.5
0.00075	27.2	26.3	26.0	22.2
0.00100	20.7	20.3	20.2	18.2
0.00125	16.7	16.5	16.4	15.3
0.00150	13.9	13.8	13.7	13.1

Figure 21 presents the values predicted by the Sun equation and also the mean values reported by the RP readers. (Note that the zero amplitude points are identically equal by definition.) All empiric RP values are normalized and ordered. The RP data are based on the responses of four readers with four replications.

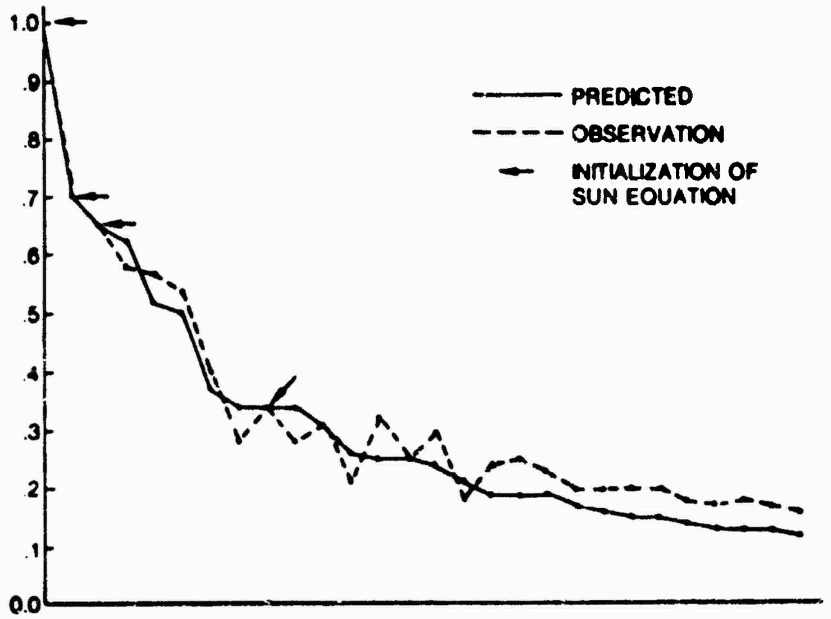

Figure 21. Modified iSL and Observed RP Values

A linear regression analysis (BMD03R, Dixon, 1977) was performed to compare the observed RP means with the Sun equation predictions for each of the 28 conditions. Very good agreement between the two data sets was obtained (correlation coefficient r = 0.99). The equation for the regression line was found to be:

$$RP = 3.89 + 0.94 \text{ (Sun equation prediction)}$$

This analysis was performed against the non-normalized cell means (collapsed across Subjects and Replications) and it is noteworthy that the intercept is less than 4 percent of maximum value. The Sun equation appears to be an excellent predictor of the effect of sinusoidal vibration (when the limiting resolution under static conditions is known a priori). Figure 22 presents the two data sets and the resulting regression equation.

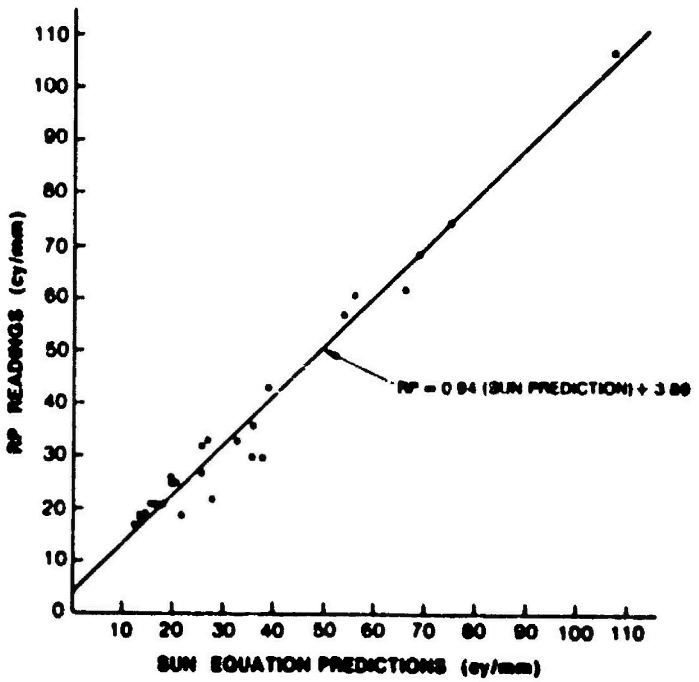

Figure 22. Regression Equation and Line of Best Fit for RP and Modified ISL Data

Visual Image Evaluation

The VIE technique and procedure were described above. Figure 23 presents the observed VIE values for the 28 experimental conditions represented in the photography. Again, as with the RP data in Figure 19, the means (collapsed across Subjects and Replicates) are plotted and the error bars represent one standard deviation.

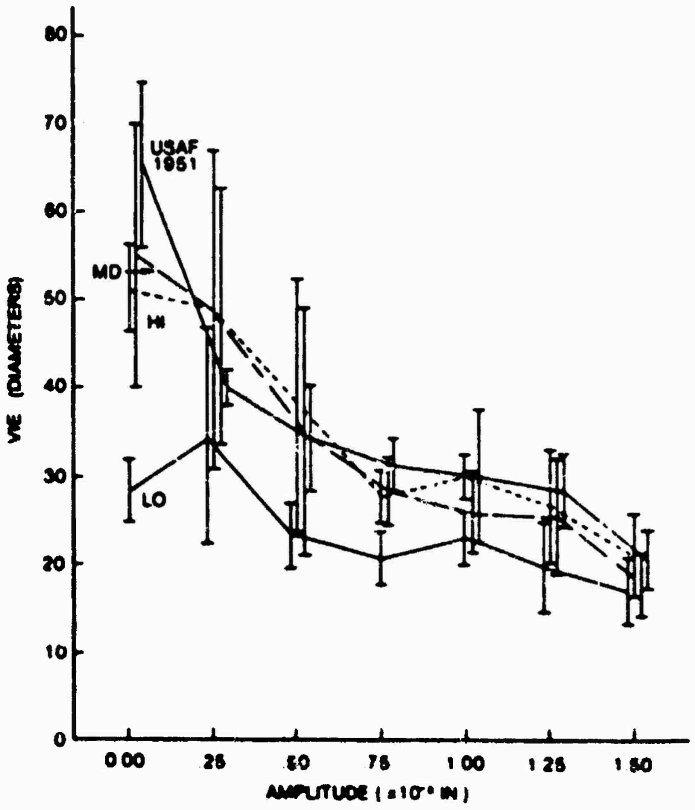

Figure 23. Observed VIE Readings

A within-subjects, repeated-measures analysis of variance (BMD08V, Dixon, 1977) was applied to the raw VIE data. The summary of this analysis is presented as Table 5. Only the third order interaction (Subjects * Targets * Ampl. ·des) was not found to be significant and only one of the three two-way interactions (Targets * Amplitudes) was not found to be highly significant. All three first order and the remaining two second order factors were found to be highly significant ($p < 0.01$). A comparison between Tables 3

and 5 is of interest since RP and VIE are both presumed to reflect image quality. For VIE, Subjects becomes a highly significant factor as do the two-way interactions which include Subjects. (The Targets × Amplitude interaction drops from being highly significant [$p < 0.01$], for RP, to being significant [$p < 0.05$], for VIE.)

An Omega-squared test (Simons, 1971) was next applied to the VIE data. The results are shown in Table 6. Over 87 percent of the total variance was accounted for by the independent variables and their interactions. In comparing Table 6 and Table 4 (RP), two differences are obvious. For the VIE, Subject differences make up 8.4 percent of the variability in the data (as opposed to 0.03 percent for RP) and the vibration amplitudes underlie 47.0 percent (as opposed to 70.8 percent) of the total variance. For VIE, sources of variance which include Subjects account for almost one-fourth of the total, while the same sources account for less than 1 percent of the experimental variability under RP. Perhaps this is due to the lack of a formal VIE training and certification procedure as exists for RP.

TABLE 5. ANALYSIS OF VARIANCE: VIE

Source	Sums of Squares	df	Mean Square	F	Significance
Subjects (S)	7797.355	3	2599.118	181.43272	**
Targets (T)	10217.48	3	3405.827	13.03676	**
Amplitude (A)	45287.25	6	7547.875	25.77972	**
S * T	2351.234	9	261.2480	18.23655	**
S * A	5270.105	18	292.7834	20.43789	**
T * A	7933.219	18	440.7344	2.73561	*
S * T * A	8699.941	54	161.1100		
Within Repetition	4813.375	336	14.32552		

*p = .05

**p = .01

TABLE 6. OMEGA-SQUARED TEST: VIE

Source	Percent of Total Variance Accounted for
Targets (T)	10.2
Subjects (S)	8.4
Amplitudes (A)	47.0
T × A	5.4
T × S	2.4
S × A	5.4
T × S × A	8.6
Total	87.4

Tukey's HSD test was also applied to the VIE data (Roscoe, 1975). For the main effect of Subjects, S_2 was significantly different ($p < 0.05$) from S_3 and all other subject-by-subject comparisons yielded highly significant differences. (For the RP technique, Subjects was not a significant main effect.) With regard to Targets, the highly significant ($p < 0.01$) main effect was found to be due to a highly significant ($p < 0.01$) difference between the low contrast "L" target and the other three targets. Most of the main effect of Amplitude was due to the static and 0.00025-inch levels being highly significantly different ($p < 0.01$) from the remaining five levels of this variable. (The significant interactions reflect the generally noisy nature of the VIE data and will not be discussed further.)

Comparison of VIE and RP Observations

Mean VIE and RP observations are presented in Figure 24. The RP values were ordered and normalized. The corresponding VIE readings were also normalized. The general trend is the same for the two curves, with the VIE data being "noisier" in the comparison. A quantitative comparison, using a linear regression analysis (BMD03R, Dixon, 1977), was applied to the paired VIE and RP observations (Figure 25). The correlation coefficient was found to be $r = 0.95$ and the regression equation was:

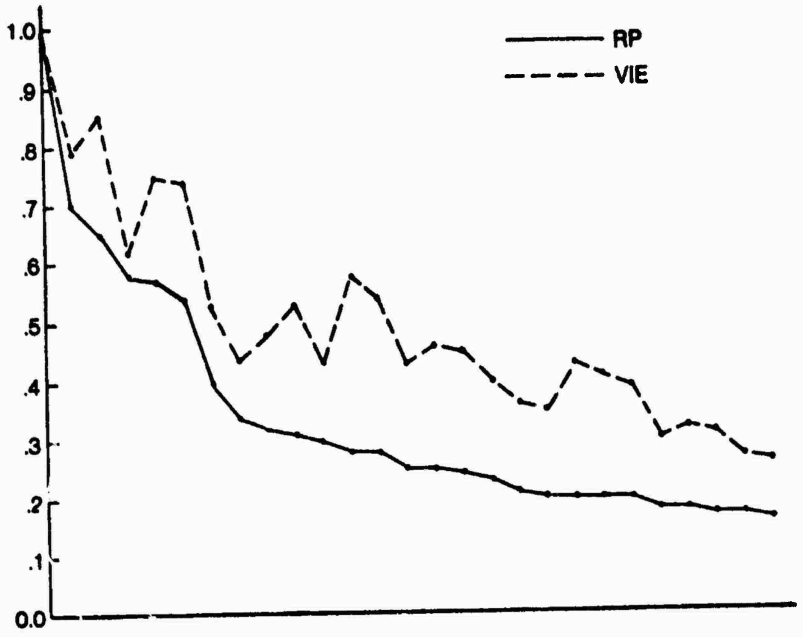

Figure 24. Observed Normalized VIE and RP Readings

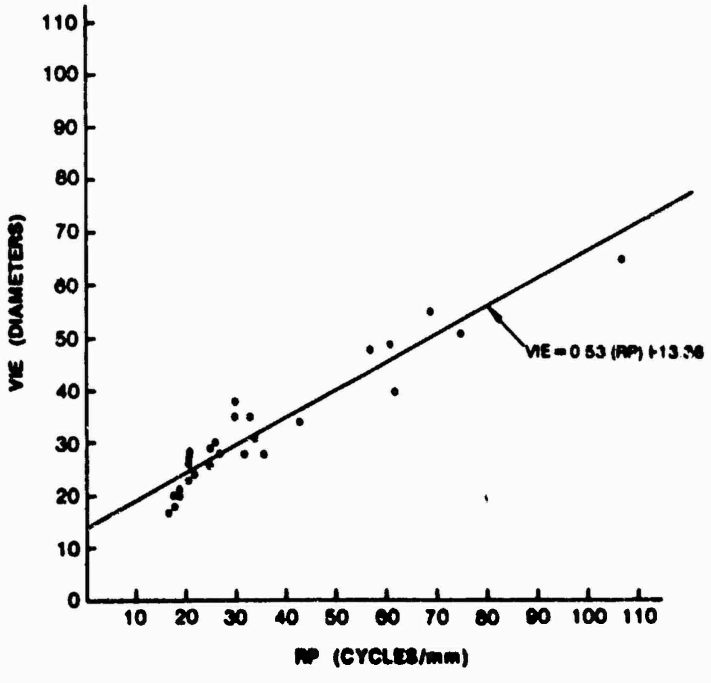

Figure 25. Regression Equation and Line of Best Fit for RP and VIE Data

$$VIE = 0.53\ (RP) + 13.36$$

By inverting this equation, VIE readings (in diameters of optical magnification) can be used to produce estimates of limiting resolution (cycles/mm):

$$RP = 1.9\ (VIE) - 25.33$$

The highly linear relationship between VIE and RP supports this computation for these experimental conditions. Operationally, the estimation of limiting resolution from VIE readings is appealing for two reasons: over 87 percent of the total variance was accounted for by the independent variables and no contrived targets are required.

Observations on Subjective Techniques

For RP results, Mayo (1968) stated that "all factors considered, no resolving power determination should be assumed more reliable than ±10 percent of the measured value, based on reader differences alone." In the present research, no significant reader differences were identified by the analysis of variance procedure. In fact, over the entire data set, the average of the standard deviations for the 28 conditions represented only slightly more than 7 percent of the grand mean. It should also be recalled that the DIA Standard requires that "the standard deviation of the differences" is less than 16 percent for RP reader certification. It appears that the DIA Standard provides reader training and criterion performance that does, in fact, effectively eliminate reader differences. In contrast, the average of the standard deviations of the VIE readings, again over the 28 conditions, represented almost 21 percent of the grand mean, and highly significant reader differences were found ($p < 0.01$). Despite the high correlation between RP and VIE ($r = 0.95$), a training and criterion demonstration program appears required before subject differences can be minimized under VIE.

OBJECTIVE

The same imagery employed in the subjective image quality assessments was scanned with a microdensitometer. The resulting digital magnetic tape recordings were subjected to four computer-implemented image assessment techniques: acutance, edge width (EW), reciprocal edge spread (RES), and MTF. Two different MTF computations were independently performed.

Acutance

Microdensitometry and acutance estimates were performed at the Dynamics and Environmental Evaluation Branch of the Air Force Avionics Laboratory (AFAL/RWF). Stanzione (1979) described the acutance procedure as follows:

> Edge data tape [is] run through [the] RWF Acutance Program, AEDGA. Data is smoothed and edge location determined, using a linear regression technique. Acutance formula used is standard SPSE [Thomas, 1973] acutance.

One photograph (of the four replicates) was selected for microdensitometric scanning. An edge, formed by one side of one of the largest bars and the adjacent background, was selected for scanning. Each edge was scanned 12 times, six partially overlapping scans in each of two opposite directions of stage travel. Between two and four of those scans were selected for each of the 28 experimental conditions. Each scan was then individually processed (as above) and the resulting acutance values were averaged (within each cell of the design, resulting in 28 observations. The use and reporting of an average acutance value appears to be the general practice (Kress and Gliatti, 1977). (Any investigation into the merit of this practice is beyond the scope of the current research.)

Figure 26 presents the averaged acutance values, arranged by Target for each Amplitude level. These data are far less orderly than the RP data shown in Figure 19.

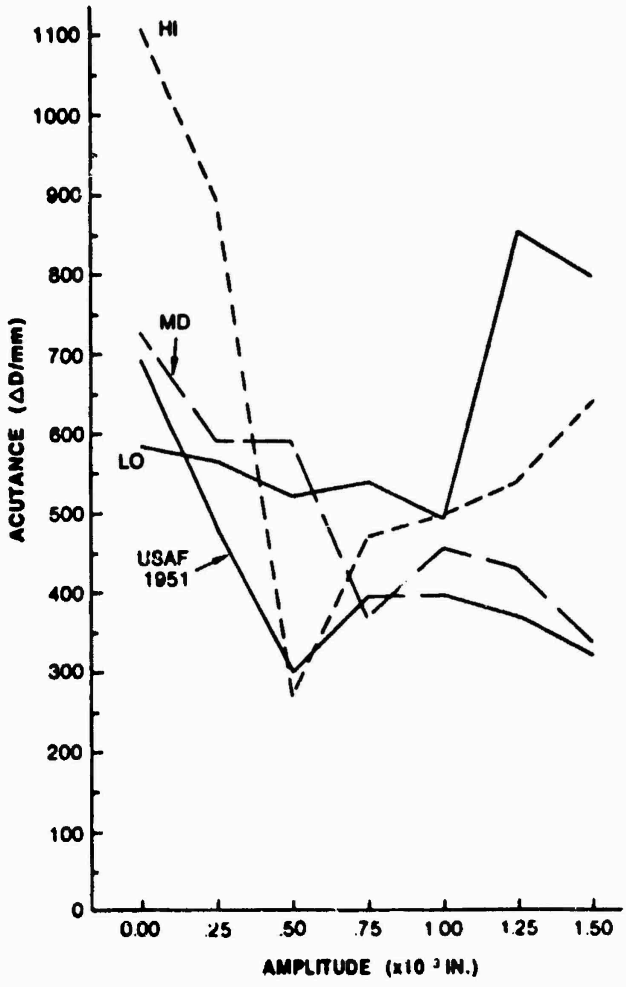

Figure 26. Observed (Mean) Acutance Values

Comparison of Acutance and RP Observations

Mean acutance and RP data are presented graphically in Figure 27. Each set was first normalized and the paired observations at each of the 28 conditions was ordered such that the RP values were in descending sequence. The acutance values do not appear to track the RP curve particularly well.

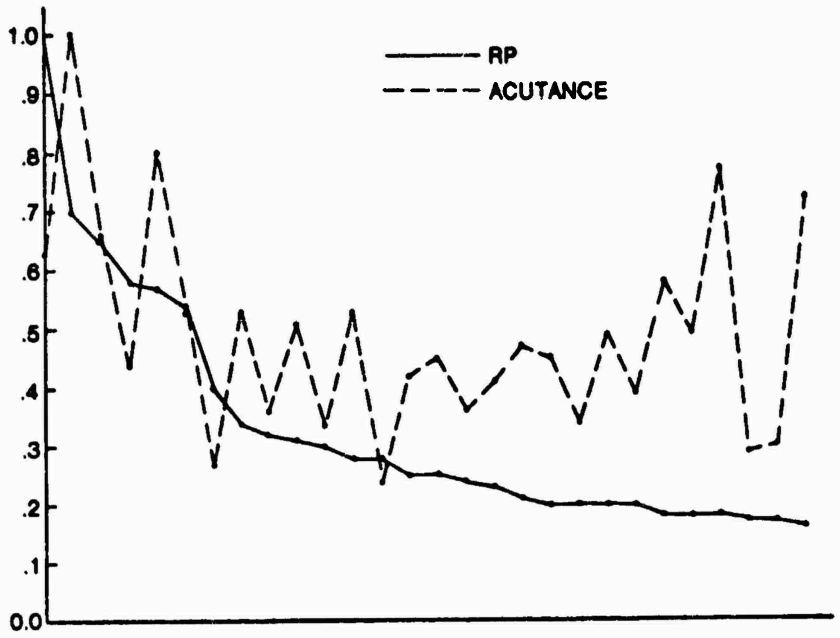

Figure 27. Mean Acutance vs. Mean RP Values

A linear regression analysis (BMD03R, Dixon, 1977) was carried out for the paired mean acutance and RP observations (Figure 28). The correlation coefficient was found to be r = 0.45, which does not suggest that a strong linear relationship exists between these two techniques. The regression equation for the line of best fit was found to be:

$$\text{Acutance} = 4.02(\text{RP}) + 401.28$$

Edge Width and RES

Stanzione (1977) noted that the "edge width reported is the width between [the] starting and stopping points used in [the] acutance calculation." These endpoints of the edge are, then, determined and the number samples between them is multiplied by the sample spacing, in microns, of the microdensitometer setup used in recording the edge scan. RES is computed from each edge width by multiplying its reciprocal by 1000 (microns per millimeter) to obtain limiting resolution (in cy/mm). The same scans were used

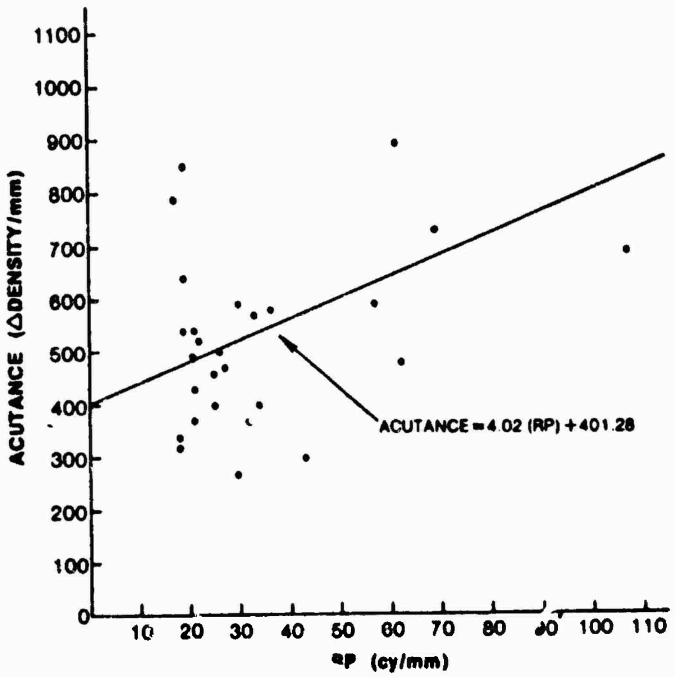

Figure 28. Regression Equation and Line of Best Fit for Acutance and RP Data

for edge width and RES calculations as were used in the acutance measurements. Figures 29 and 30 present mean, normalized edge width and RES data with respect to the RP baseline.

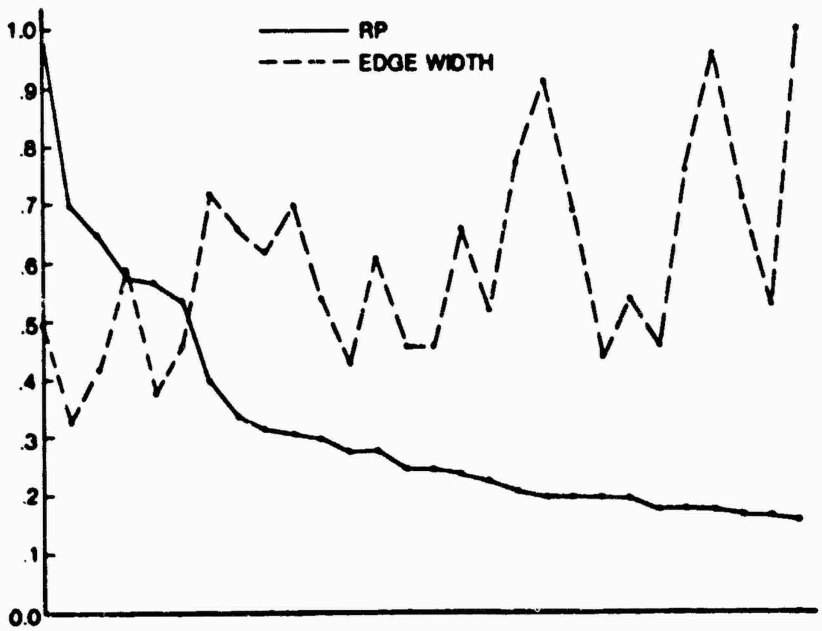

Figure 29. Mean Edge Width vs. Mean RP Values

Figure 30. Mean RES vs. Mean RP Values

Comparison of Edge Width and RES to RP

Linear regression analyses (BMDO3R, Dixon, 1977) were carried out comparing edge width and RES to RP. For edge width, the correlation coefficient was found to be r = -0.46 and the equation for the line of best fit was:

$$\text{Edge Width} = -0.25\ (\text{RP}) + 48.98$$

For RES, r = 0.50 and the equation was:

$$\text{RES} = 0.17\ (\text{RP}) + 20.77$$

Neither of these two techniques compared well with respect to RP. (See Figures 31 and 32.)

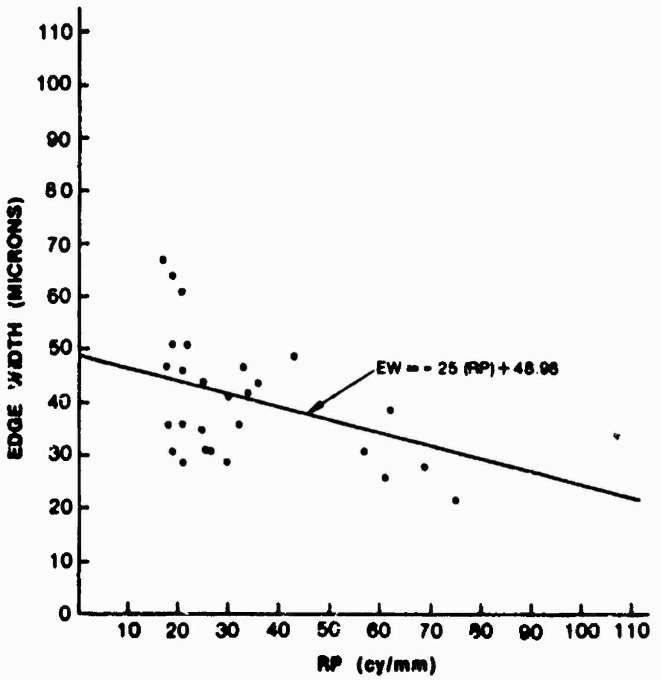

Figure 31. Regression Equation and Line of Best Fit for Edge Width and RP Data

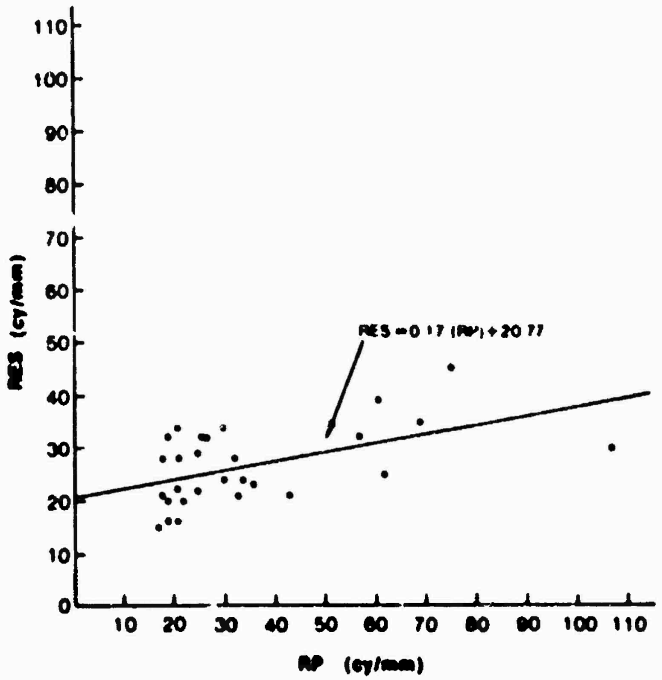

Figure 32. Regression Equation and Line of Best Fit for RES and RP Data

MTF

Two MTF analysis packages were applied to the raw edge trace data records. The first was developed and is maintained by AFAL/RWF; the second was a program developed by Mead Technology Laboratories, Inc. (MTL), Dayton, Ohio, procured for this study on a commercial services basis. Microdensitometry was performed at AFAL/RWF. The same scans were used for MTF estimates as were used for acutance, edge width, and reciprocal edge spread. The microdensitometer scans were edited by AFAL in a preprocessing step. First, only the odd-numbered microdensitometer scans were retained for each edge to avoid any misalignment caused by the alternating direction of the microdensitometer stage travel during digitizing. Second, the remaining scans were manually edited to remove any data that were possibly contaminated by artifacts (such as emulsion scratches, microdensitometer malfunctions, or operator errors). A total of 74 sets of six scans was produced to encompass the 28 experimental treatment combinations. (Each Target × Amplitude combination was represented in the microdensitometric data by at least one and at most four sets of scans.)

AFAL/RWF used all 74 digital records. The six scans corresponding to a treatment condition were averaged and processed through their program AEDGA. Where replicate data sets were available for a treatment condition, each (averaged) set was processed separately and the limiting resolution was estimated by the MTF/AIM method. The published AIM curve was adjusted to the gamma (slope) of the film processing curve representative of the actual photography. It was also adjusted to the modulation for that specific photograph following the procedure in Brock, et al. (1966). For each experimental condition, if replicate data sets existed, the average limiting resolution was provided.

Figure 33 presents the limiting resolutions estimated by the AFAL MTF procedure. No variability about the mean information was provided, in keeping with operational practice.

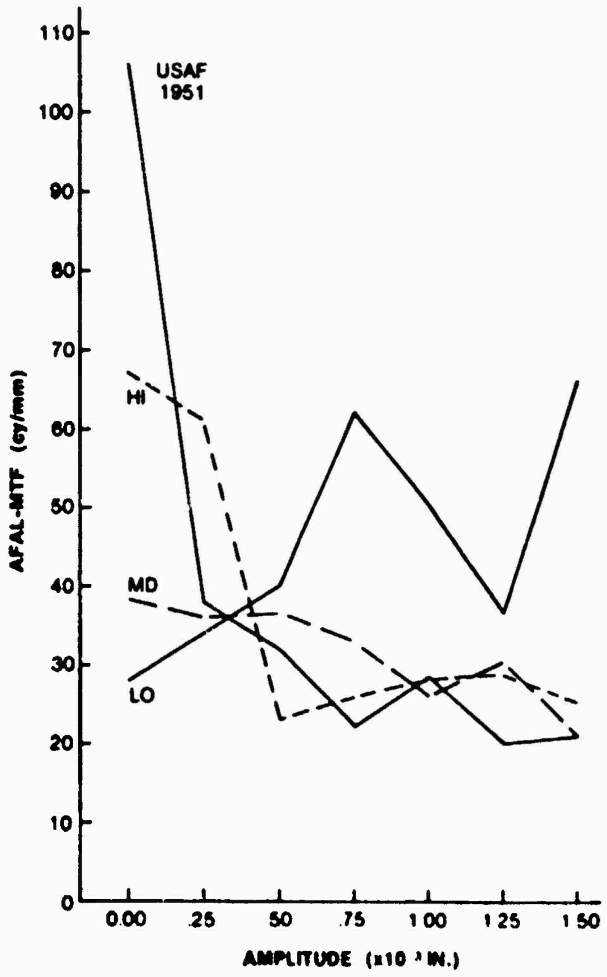

Figure 33. Observed MTF/AIM Intercepts (AFAL)

MTL selected one set of the six microdensitometric scans for each of the 28 experimental conditions. Ream (1979) reported that "three of the images . . . [the low contrast target at 0.00025, 0.00050, and 0.00150 inch amplitudes] . . . were deemed not suitable for analysis, in that the edge limits could not be established." The remaining 25 data sets were each averaged and computer analyzed to yield MTF estimates. The AIM curve data were adjusted (as above) to yield estimates of the limiting photographic system resolution.

Figure 34 presents the results of the MTL analysis. Each of the 25 plotted points represents a single MTF/AIM observation.

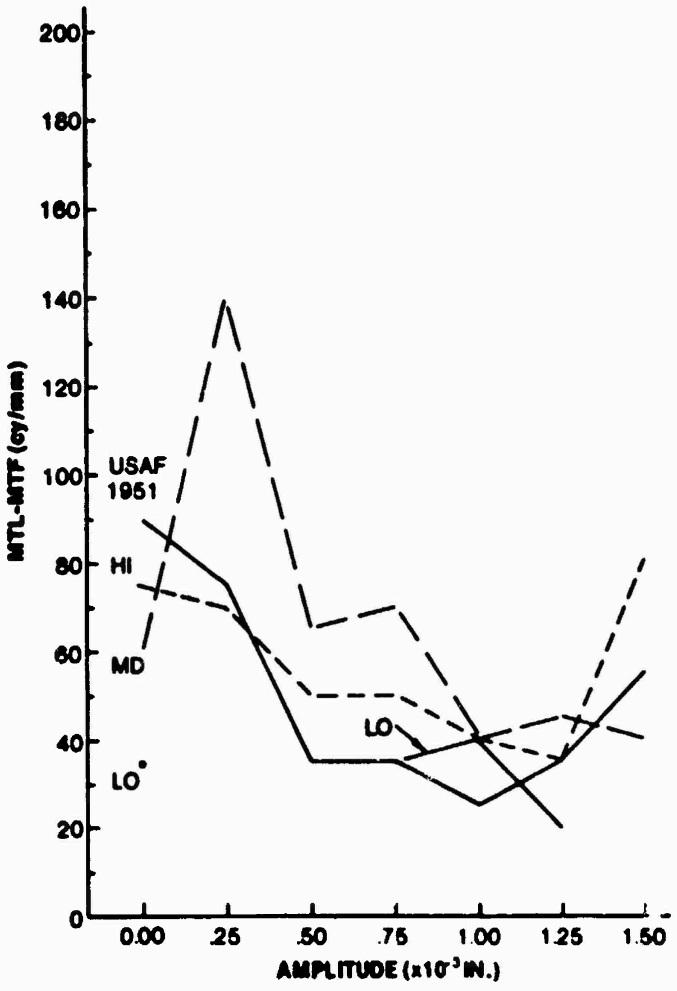

Figure 34. Observed MTF/AIM Intercepts (MTL)

Comparison of MTF/AIM and RP Observations

Mean (or single observation) MTF/AIM estimates of limiting resolution by AFAL and MTL are shown graphically in Figures 35 and 36 versus the mean RP data. In each case, the data pairs are normalized and ordered according to the descending RP values.

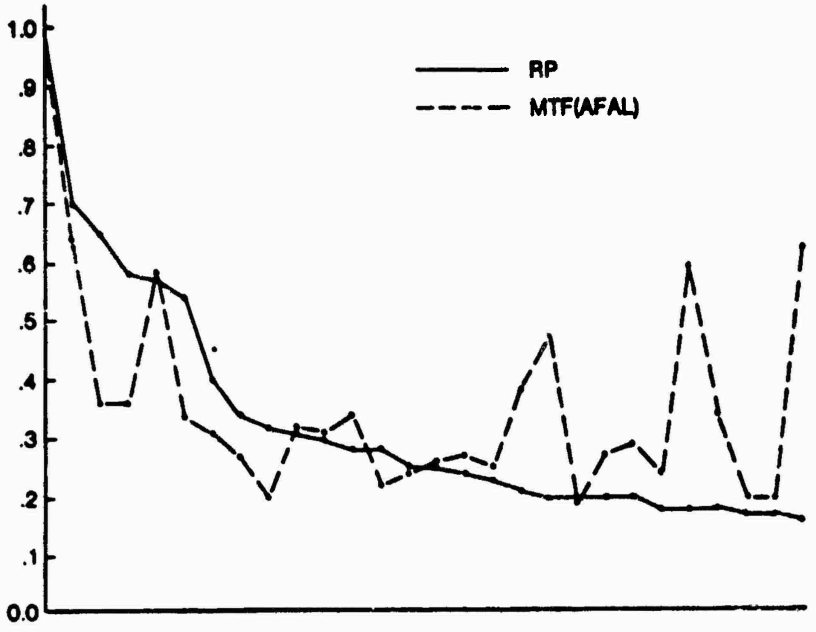

Figure 35. Observed Normalized MTF/AIM (AFAL) and RP Estimates

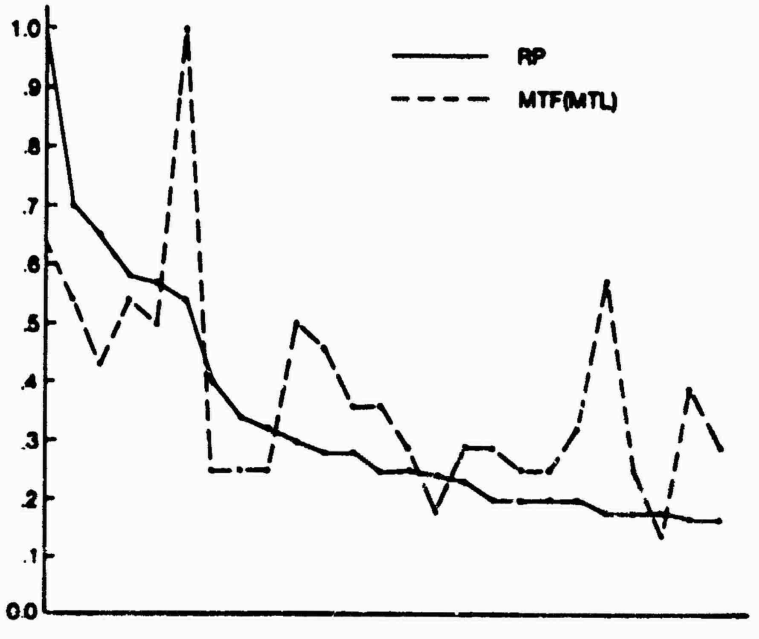

Figure 36. Observed Normalized MTF/AIM (MTL) and RP Estimates

Linear regression analyses (BMD03R, Dixon, 1977) were applied to the two sets of MTF/AIM data. Twenty-eight paired observations were available for the AFAL-produced data, while only 25 pairs existed for the data generated by MTL. The correlation coefficient for the AFAL data (versus mean RP) was r = 0.64 and the equation of the line of best fit was found to be:

$$\text{MTF/AIM (AFAL)} = 0.56\ (\text{RP}) + 18.19$$

The correlation coefficient for the MTL data (versus RP) was found to be r = 0.60 and the equation of the line of best fit was:

$$\text{MTF/AIM (MTL)} = 0.68\ (\text{RP}) + 28.63$$

The AFAL and MTL MTF/AIM versus RP comparisons are shown in Figures 37 and 38.

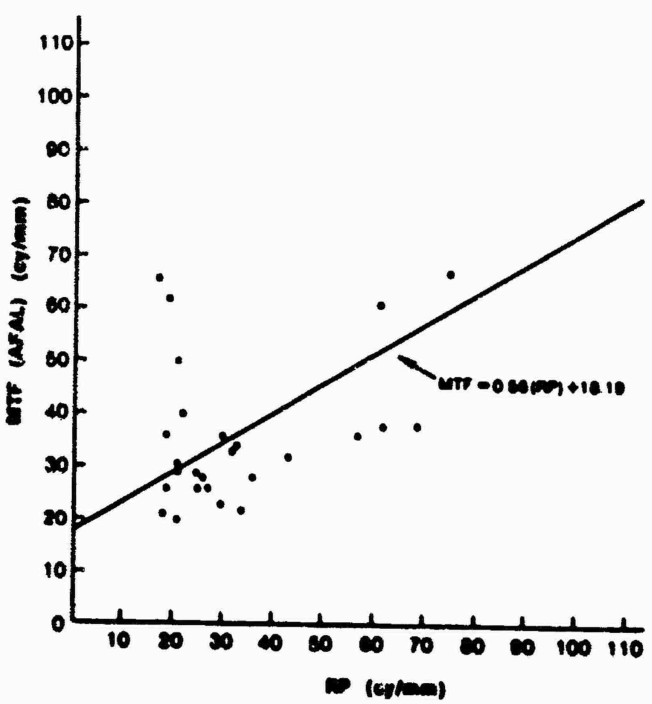

Figure 37. Regression Equation and Line of Best Fit for AFAL MTF/AIM and RP Estimates

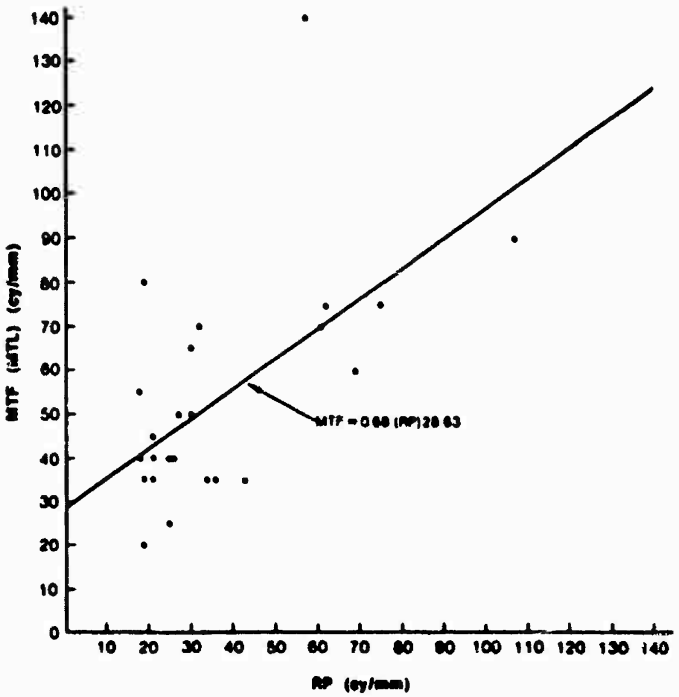

Figure 38. Regression Equation and Line of Best Fit for MTL MTF/AIM and RP Estimates

Comparison of MTF/AIM and Modulation

Because of the relatively poor linear fits observed between the two MTF/AIM estimates and the baseline RP readings, it was decided to investigate the modulation of the photography as a possible cause of the lack of agreement. The rationale for this analysis was to determine if a confound had been introduced by fluctuations in modulation across the Target × Amplitude conditions beyond the independent variable. This was carried out by performing a regression analysis of each MTF/AIM data set against the appropriate measured target modulations (Section 5). Poor agreement was observed. The correlation coefficients for the AFAL and MTL data versus modulation were r = 0.33 and 0.43, respectively. A second, intuitive, analysis, based on the shape of the edge was also carried out and is presented below.

Effects of Edge Shape on Objective Measures

The MTF estimation is based on the spatial frequency content of an edge image while the acutance and edge width estimates are based on the spatial distribution of density (or exposure) values across the edge. The physical description of the edge image, under motion degradation, merits discussion.

For the static case, an edge target in transmittance is recorded as an edge, i.e., a Heaviside function in exposure. If linear image motion were applied during the exposure interval, then the exposure distribution becomes time dependent. Figure 39A shows the illumination distribution I(x) for an edge with respect to distance X. Figure 39B shows the effect of linear motion with velocity V during an exposure period (shutter open) T. Figure 39C shows the resulting exposure distribution E(x) recorded on the film. The exposure distribution which results from perturbing an edge target with linear image motion is a ramp.

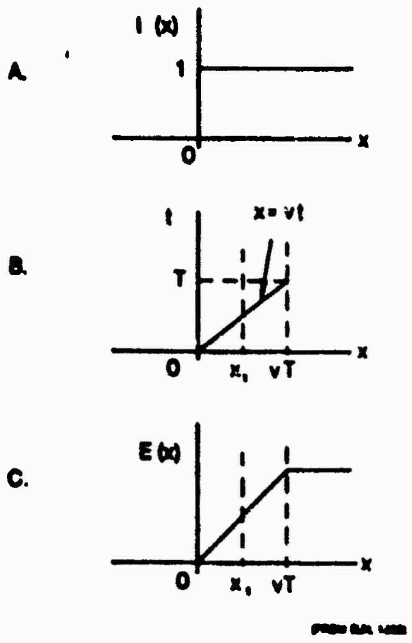

Figure 39. Linear Image Motion

The effect on the exposure distribution resulting from applying (an integral number of cycles of) sinusoidal motion to an edge during the shutter open period is depicted in Figure 40. Figure 40A is, again, an edge, and Figure 40B shows the image excursion during one full cycle of the sinusoid (of frequency f cycles per second and amplitude 2b). Figure 40C shows the exposure resulting from the first quarter cycle of the sine wave and Figure 40D depicts the exposure distribution resulting from a complete cycle. (Sun, 1966, presents the exposition from which the above figures were adopted in terms of integral equations, while Rosenau, 1963, employs modulation transfer functions in providing an analytic development of image motion effects on photographic system performance.)

Figure 40D presents the exposure distribution of an edge after induced sinusoidal motion. It does not exhibit film grain noise effects, and the endpoints of the degraded edge are clearly defined. The MTF, based on the spatial frequency content of the image, receives its highest spatial frequency information from the portions of the exposure distribution closest to these endpoints, i.e., where the rate of change in exposure with respect to distance is greatest.

Acutance is based on the rate of change in density with respect to distance. Density D is defined as follows:

$$D = -\log_{10} T$$

where T is the percent transmittance of the image and is measured on a calibrated microdensitometer. (The relationship between density and exposure is a function of the film/processing combination and was shown for the present case in Figure 10.) Higher acutance values will result from sharper edges (less distance) and increased modulation (greater density difference). Again, the portions of the edge closest to the endpoints contribute strongly to higher acutance values. Unfortunately, photographic systems are noisy, with noise arising from the number and size distribution of silver halide grains and being proportional to the average density level. Microdensitometric sampling is susceptible to noise in the image, with small apertures (required to achieve high spatial frequency response) being most sensitive

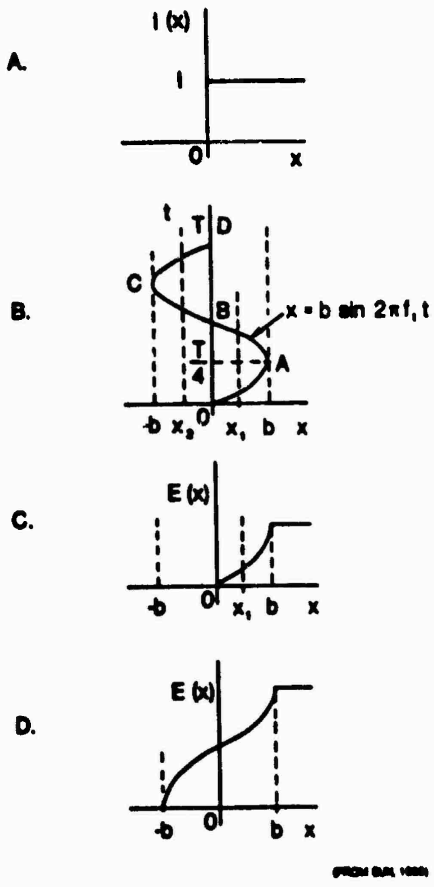

Figure 40. Sinusoidal Image Motion

to grain fluctuation. (See Figure 41.) Both techniques, acutance and MTF, are sensitive to information in the sampled edge exposure/density distribution immediately interior to the edge endpoints. Endpoint location, particularly in the presence of grain noise, is a critical and nontrivial task, as can be seen from Figure 42, a single microdensitometer scan plotted for an edge selected from a USAF 1951 target image under static conditions.

The selection of endpoints from the sinusoidal motion-degraded, noisy, edge target microdensitometer scans appears to be particularly difficult. Ream (1979) found it impossible for almost 11 percent of the conditions; the missing data points from the MTL analysis were all at low target contrast. Errors in endpoint location can produce disproportionate changes in the

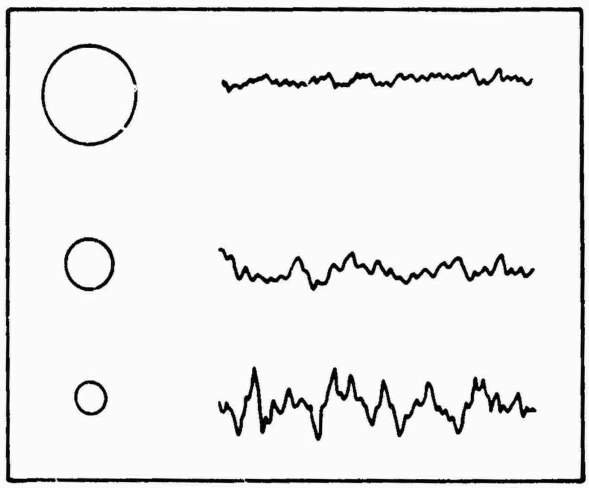

(FROM DAINTY AND SHAW, 1974)

Figure 41. Relationship Between Aperture Size and Density Fluctuation During Image Scanning

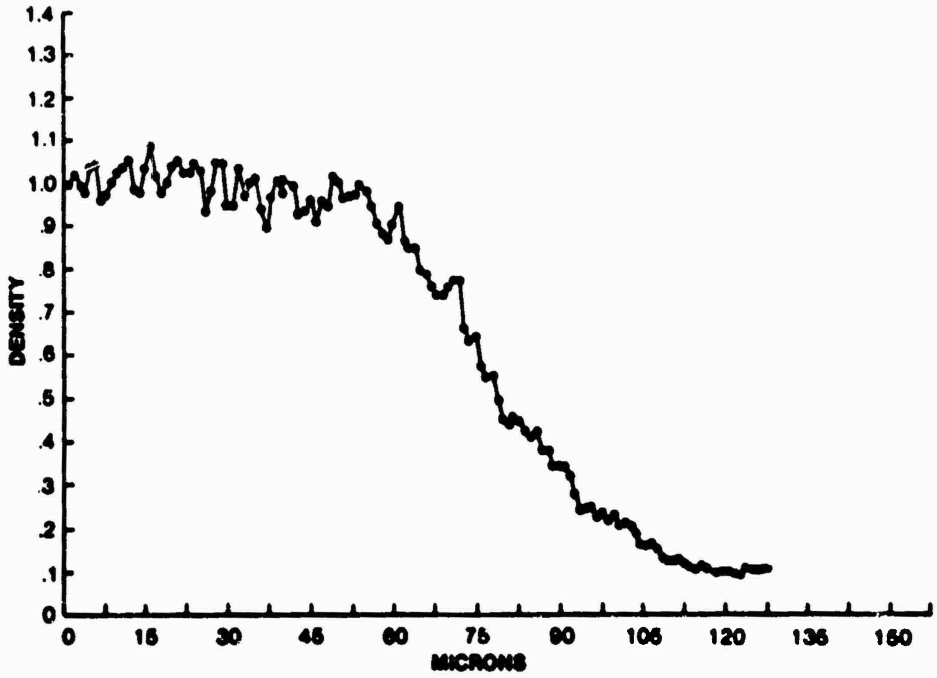

Figure 42. Plot of Single Microdensitometer Scan

computed MTF and acutance estimates because of the sensitivity of these techniques to the edge shape in the immediate vicinity of the endpoints.

Comparison of Image Quality Assessment Techniques

In order to perform a general comparison across all the image quality assessment techniques, a test of the significance of the difference between two correlation coefficients for correlated samples (Ferguson, 1971) was employed. This statistic can be used when three measurements (at least) have been made on the same process. The three measurements (M_1, M_2, and M_3) yield three correlation coefficients (r_{12}, r_{13}, and r_{23}) when pairwise comparisons are made between the measurements. This statistic permits pairwise comparisons between r_{12}, r_{13}, and r_{23}. In the present application, the RP measurement technique was used as a reference, in that the correlation coefficients r_{ij} were each developed by comparing the measurement technique M_i to the RP data. For example, in order to compare RES and VIE, the correlation coefficients for RES with respect to RP and for VIE with respect to RP, are compared against each other.

Table 7 summarizes the comparison of the nine image assessment techniques and models. In each case, the correlation coefficient shown in the table is derived with respect to RP.

TABLE 7. PAIRWISE COMPARISON OF CORRELATION COEFFICIENTS

Technique	Correlation Coefficient
Sun's equation	0.99
ISL	0.96
MTF	0.96
VIE	0.95
MTF/AIM (AFAL)	0.64
MTF/AIM (MTL)	0.60
RES	0.50
Edge Width	-0.46
Acutance	0.45

(The edge width technique can be ignored because it is reciprocally related to RES.) As indicated by the joined arrows, the techniques fell into three highly significantly different ($p < 0.01$) groups. The Sun model, a version of ISL using static condition observations to base prediction of dynamic performance, was in a group by itself. Because of the high value of the correlation coefficient, it was, then, the best correlate to RP. A second group was made up of the ISL and MTF predictions and the VIE subjective observations; these three measurements were not statistically different from each other as correlates to RP. This second group also showed excellent agreement with RP. The last group was made up of four (ignoring edge width) objective measures: acutance, RES, and the two MTF/AIM methods. These objective measurement techniques were not significantly different from each other, with respect to RP, nor were they good correlates of the RP baseline data.

Section 7
CONCLUSIONS

1. The MTF and ISL models for predicting limiting resolution are essentially identical in their results (r = 0.998). The MTF model is the more conservative predictor.

2. The RP technique is an excellent estimate of image quality (limiting resolution). This is borne out by the very close agreement obtained in comparing RP to the two analytically based models (r = 0.96) and by the fact that the RP measure accounted for more than 96 percent of the total experimental variance.

3. The correction of RP based on the input target modulation (Mayo, 1968) failed to produce the desired results. Two causes of this failure suggest themselves--first, that the lowest modulation targets (low contrast "L") were outside the range of the formula and, second, that the formula is not appropriate for imagery that has been degraded by sinusoidal motion.

4. Both the ISL and MTF models are good predictors of RP (r = 0.96 for each comparison).

5. Sun's extension (1967) to the ISL model, using static RP observations to initialize the computation, produced predictive results that were in excellent agreement (r = 0.99) with the RP baseline.

6. The VIE technique is a very good measure of image quality, accounting for over 87 percent of the experimental variance and exhibiting a highly linear relationship (r = 0.95) when compared to the RP reference.

7. All objective techniques (MTF/AIM [AFAL], MTF/AIM [MTL], acutance, edge width, and RES) showed good agreement with each other (Table 7) but poor agreement with RP (r between 0.45 and 0.64). It is suspected, at least for the conditions of this experiment, that these techniques are sensitive to the accuracy of edge endpoint selection and that for sinusoidal motion-degraded photographs, this selection is difficult to perform.

APPENDIX

ADDITIONAL RP ANALYSES

The comparison of image quality estimators developed in the main body of this report was based on correlational analyses performed between pairs of estimators. If a single technique were being employed to evaluate a camera system, then a more detailed statistical analysis should be carried out. This appendix provides such treatment for RP.

In the foregoing analysis of variance (Section 6), it was found that only three of the four target contrast levels were significantly different from each other. The high and medium contrast target conditions were not distinguishable from each other. It was decided, therefore, to collapse these two conditions into a single level of Target. Figure A-1 presents the results of this pooling in graphic form. The error bars denote one standard deviation above and below the mean at each Amplitude level.

An analysis of variance for a within-subjects, repeated-measures design (BMD08V, Dixon, 1977) was applied to the raw RP data. In this analysis, there were only three levels of Target: the USAF 1951, the pooled high and medium contrast, and the low contrast target levels. The same seven Amplitude levels as above were considered. Table A-1 presents a summary for this analysis. The main effects of Target and Amplitude were highly significant ($p < 0.01$), as was the Target × Amplitude interaction.

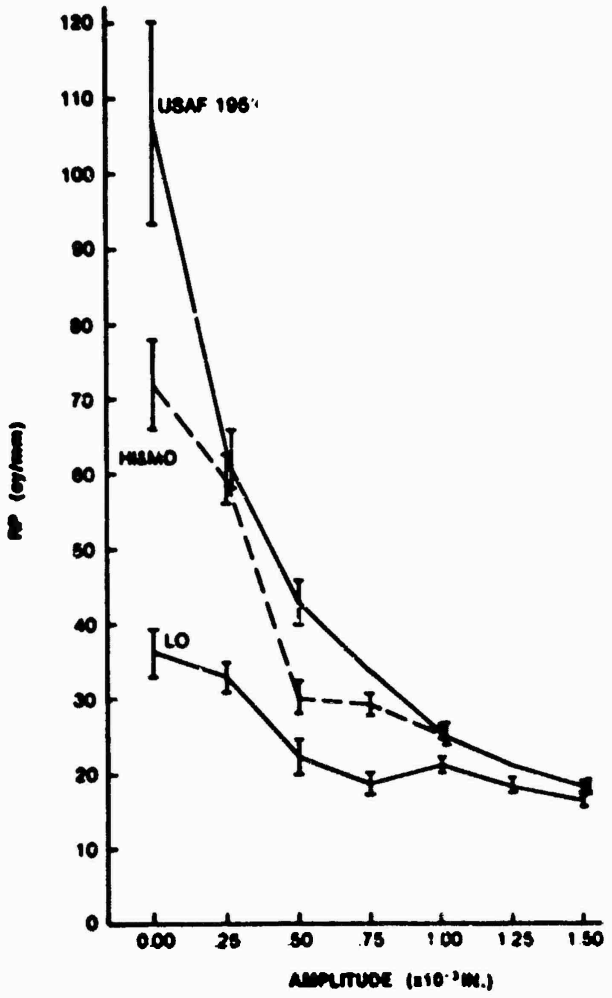

Figure A-1. Partially Pooled RP Data

TABLE A-1. ANALYSIS OF VARIANCE: PARTIALLY POOLED RP DATA

Source	Sums of Squares	df	Mean Square	F	Significance
Subjects(S)	10.13106	3	3.377021	2.524	
Targets (T)	2161.155	2	1080.577	2500.354	**
Amplitude (A)	10003.96	6	1667.327	1201.790	**
S × T	2.593018	6	0.4321696	0.323	
S × A	24.97266	18	1.387369	1.037	
T × A	2667.043	12	222.2536	195.425	**
S × T × A	40.94214	36	1.137281	0.850	
Within Repetition	337.1914	252	1.338060		

*$p \leq .01$

**$p \leq .05$

Table A-2. OMEGA-SQUARED TEST: PARTIALLY POOLED RP DATA

Source	Percent of Total Variance Accounted for
Targets (T)	14.2
Subjects (S)	0.04
Amplitude (A)	65.6
T × A	17.4
T × S	0.00
S × A	0.016
T × S × A	0.00
Total	97.25

An Omega-squared test (Simons, 1971) was applied to the partially collapsed RP data to identify the percentage of the total experimental variance accounted for by each factor/combination (Table A-2). The independent variables and their interactions accounted for over 97 percent of the total variability in the observed data. The three highly significant factors also accounted for over 97 percent of the experimental variance.

The two factors and their interaction, for which significant effects were determined, were subjected to additional scrutiny in the form of Tukey's HSD (Roscoe, 1975). All three levels of Target were now found to be highly significantly different ($p < 0.01$) from each other. With regard to Amplitude, only the two greatest excursions (0.00125 and 0.000150 inch displacements) were not significantly different from each other and only the 0.00075 and 0.00100 inch displacement comparison yielded a difference significant at $p < 0.05$; all other pairwise Amplitude combinations produced highly significant ($p < 0.01$) differences. The results of applying Tukey's HSD to the Target × Amplitude interaction are shown tabularly in Table A-3. The table is arranged in a fashion akin to a Newman-Keuls table in that the subject combinations have been arranged in order by increasing RP value.

TABLE A-3. TUKEY'S HSD ON TARGET × AMPLITUDE INTERACTION FOR PARTIALLY POOLED RP DATA

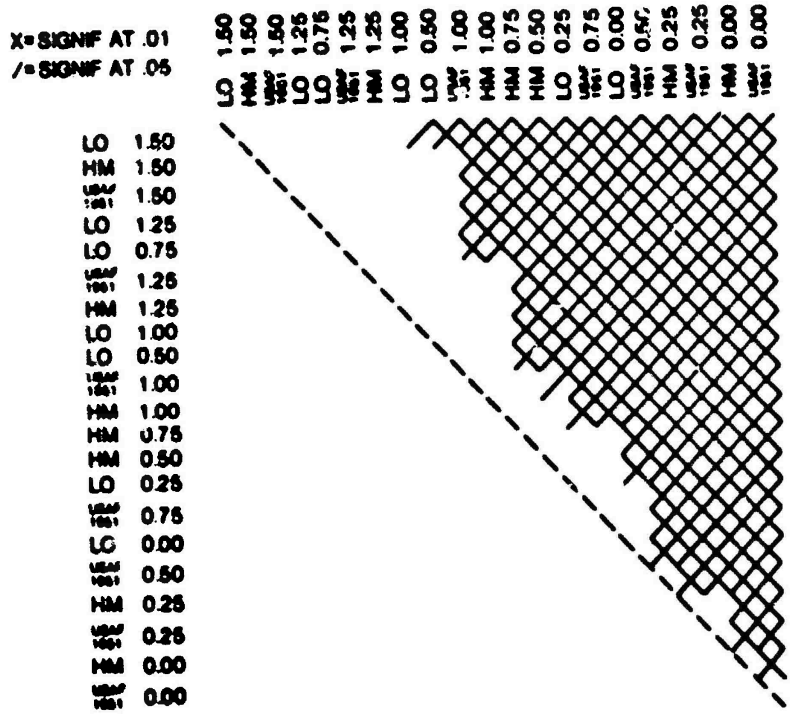

REFERENCES

Air Force Avionics Laboratory, 15 September 1973, Controlled Range Network (CORN) Manual. Air Force Avionics Laboratory, Wright-Patterson Air Force Base, Ohio.

Attaya, W. L., Brock, G. C., et al., November 1966, Study of Image Evaluation Techniques (Technical Report AFAL-TR-66-343). Air Force Avionics Laboratory, Wright-Patterson Air Force Base, Ohio.

Attaya, W. L., & Yachik, T. R., February 1971, Photographic Quality Transfer Techniques (Technical Report 71-9651-1). Lexington, Mass.

Berkovitz, M. A., February/March 1969, Determining Resolution of Photo-Optical Systems. Image Technology.

Biberman, L. M., 1973, Image Quality. In Perception of Displayed Information. Plenum Press, New York.

Brock, G. C., 1967, The Physical Aspects of Aerial Photography. Dover Publications, Inc., New York. (a)

Brock, G. C., 1967, Reflections on Thirty Years of Image Evaluation. Photographic Science and Engineering, 2(5). (b)

Brock, G. C., 1970, Image Evaluation for Aerial Photography. Focal Press, London.

Brock, G. C., et al., May 1963, Study of Image-Evaluation Techniques (Interim Engineering Report 9048-3). Itek Corporation, Lexington, Mass.

Brock, G. C., Harvey, D. I., Kohler, R. J., & Myskowski, E. P., 1966, Photographic Considerations for Aerospace (2nd ed.). Itek Corporation, Lexington, Mass.

Burke, R., Marshall, W., & Keane, J., September 1974, Photographic Systems Performance Analysis Using Double-Annulus Targets (AFAL-TR-74-218). Air Force Avionics Laboratory, Wright-Patterson Air Force Base, Ohio.

Charman, W. N., & Olin, A., 1965, Image Quality Criteria for Aerial Camera Systems. Photographic Science and Engineering, 9(6).

Coltman, J. W., 1954, The Specification of Imaging Properties by Response to a Sine Wave Input. Journal of the Optical Society of America, 44.

Cooley, J. W., & Tukey, J. W., 1965, An Algorithm for the Machine Computation of Complex Fourier Series. Mathematics of Computers, 19.

Crane, A. C., Jr., December 9-11, 1975, Status of Project Sentinel Sigma. Minutes of the Third Sentinel Sigma Image Evaluation Workshop, Wright-Patterson Air Force Base, Ohio.

Crane, A. C., Jr., February 22-28, 1975, Air Force Image Quality Control Program. Proceedings of the American Society of Photogrammetry, 42nd Annual Meeting, Washington, D.C.

Dainty, J. C., & Shaw, R., 1974, Image Science. Academic Press, New York.

Defense Intelligence Agency, 12 June 1975 (including changes through February 1978), DoD Exploitation of Multisensor Imagery (DIAM 57-5). Defense Intelligence Agency, Washington, D.C.

Defense Intelligence Agency, 1975, Standardized Assessment and Expression of Tribar Resolution. Defense Intelligence Agency, Washington, D.C.

Department of Defense, 12 May 1959 (including changes through 28 January 1963), Photographic Lenses (Military Standard MIL-STD-150A). U.S. Government Printing Office, Washington, D.C.

Department of Defense, December 1967, Image Interpretation Handbook (Vol. 1) (Air Force Manual AFM 200-50). U.S. Government Printing Office, Washington, D.C.

Department of the Air Force, 10 January 1975, Mapping, Charting, and Geodesy: Quality Control Requirement for Continuous Photographic Processing Laboratories (Air Force Regulation AFR 96-1).

Department of the Air Force, November 1978, Photographic Processing Facilities (Vol. 2): The Quality Control System (Technical Manual T.O. 10-1-6-2). (Draft revision to Section 13, "Imagery Evaluation"). Washington, D.C.

Dixon, W. J. (Ed.), 1977, BMD: Biomedical Computer Programs. University of California Press, Berkeley.

Ferguson, G., 1971, Statistical Analysis in Psychology and Education (3rd ed.). McGraw-Hill, New York.

Fraggiotti, J., 22 August 1979, Effects of Vibration on Photographic Systems (Report No. 6481-79-01). Systems Research Laboratories, Inc., Dayton, Ohio.

Fryer, M. J., October 1977, A Technique for Obtaining Film Threshold Modulation (Technical Memorandum IT 166). Royal Aircraft Establishment, London.

Gliatti, E. L., 1977, Modulation Transfer Analysis of Aerial Imagery. Photogrammetria, 33.

Gliatti, E. L., 28-29 March 1978, Image Evaluation Methods. Proceedings of the Society of Photo-Optical Instrumentation Engineers (Vol. 137): Airborne Reconnaissance III. Washington, D.C.

Gold, B., & Rader, C. M., 1969, Digital Processing of Signals. McGraw-Hill, New York.

Higgins, G. C., 1977, Image Quality Criteria. Journal of Applied Photographic Engineering, 3(2).

HRB-Singer, Inc., 19 January 1971, Preliminary Examination of a Magnification Concept for Evaluating Photographic Imagery. HRB-Singer, Inc., Rome, New York.

Jensen, N., 1968, Optical and Photographic Reconnaissance Systems. John Wiley, New York.

Katz, A. H., September 1963, On the Informal History of Image Evaluation Techniques and Practice (Rand Paper P-2789). The Rand Corporation.

Kress, B. A., & Gliatti, E. L., September 1977, General Procedures for Acquisition, Processing, and Analysis of Microdensitometer Data. Air Force Avionics Laboratory, Wright-Patterson Air Force Base, Ohio.

Kuperman, G. G., November 1966, Controlled Range Network Photometric Camera Calibration (Technical Note DTN-66-7). Data Corporation, Dayton, Ohio.

Loosberg, P., September 1972, Micro-Analyzer Support (AFAL-TR-72-300). Air Force Avionics Laboratory, Wright-Patterson Air Force Base, Ohio.

Mayo, J. W., III., 9 August 1968, Photographic Resolving Power of Aerial Lenses as a Function of Target Modulation (Technical Report 28). The University of Arizona, Tucson.

Noffsinger, E. B., 1970, Image Evaluation: Criteria and Applications. S.P.I.E. Journal, 9.

Pittman, G., July 1965, Statistical Analysis of Emulsion Resolving Power Threshold Data. In Study of Image-Evaluation Techniques (Interim Engineering Report 65-9048-13). Itek Corporation, Lexington, Mass.

RCA, 1974, Electro-Optics Handbook. (RCA Technical Series EOH-11).

Ream, J., 20 August 1979, MTF Analysis of 3404 Images (Technical Memorandum). Mead Technology Laboratories, Inc., Dayton, Ohio.

Rodriguez-Torres, C., & Summers, R. B., March 1976, Photographic Emulsion Threshold Functions Study (AFAL-TR-76-19). Air Force Avionics Laboratory, Wright-Patterson Air Force Base, Ohio.

Roetling, P. G., Trabka, E. A., & Kinzly, R. E., 1968, Theoretical Prediction of Image Quality. Journal of the Optical Society of America, 58(3).

Roscoe, J. T., 1975, Fundamental Research Statistics for the Behaviorial Sciences (2nd ed.). Holt, Rinehart, and Winston, New York.

Rosenau, M. D., Jr., 6 March 1963, Image-Motion Modulation Transfer Function. Modulation Transfer Function Symposium, Norwalk, Conn.

Saunders, K., 1970, Concept for Rapid Evaluation of High Resolution Photography. Washington, D.C.

Scott, Frank, 1968, The Search for a Summary Measure of Image Quality--A Progress Report. Photographic Science and Engineering, 12(3).

Selwyn, E. W. H., 1935, A Theory of Graininess. Photographic Journal, 75.

Sikora, J. J., & Kuperman, G. G., April 1970, MTF Analysis of Sample Flight Test Imagery (Technical Report DTR-70-8). Data Corporation, Dayton, Ohio.

Simons, C. W., December 1971, Considerations for the Proper Design and Interpretation of Human Factors Engineering Experiments (Technical Report No. P73-325). Hughes Aircraft Company, Culver City, Calif.

Stanzione, T., 16 August 1979, Acutance Analysis of Vibration Specimens (Technical Memorandum). Air Force Avionics Laboratory, Wright-Patterson Air Force Base, Ohio.

Sun, Y. C., December 1967, Advanced Photo Subsystem Component Analysis: Effects of Vibration and Other Random Motions on High Resolution Photography (Sinusoidal Vibration Study and Experimentation Phase) (Technical Report No. AFAL-TR-67-260). Air Force Avionics Laboratory, Wright-Patterson Air Force Base, Ohio.

Tactical Air Warfare Center, September 1972, Constant Quality. Eglin Air Force Base, Fla.

Thomas, W., Jr., (Ed.), 1973, SPSE Handbook of Photographic Science and Engineering. John Wiley & Sons, New York.

Wernicke, B. K., September 1959, Effect of Image Motion on Resolving Power Empirical Measurements with Specific Material (WADC Technical Note). Aerial Reconnaissance Laboratory, Wright-Patterson Air Force Base, Ohio.

*U.S. Government Printing Office: 1980 — 657-074/787